

CONTENTS

	<u>Page No:</u>
Introduction	1
Accelerator	2
Research Experiments	9
Instrumentation	42
Indian Nuclear Data Group	46
Seminars	47
Library	48

INTRODUCTION

The operation and utilization of the 5.5 MeV Van de Graaff Accelerator at Trombay during the period from 1st January 1967 to 30th June 1968 are covered in this report. The accelerator has completed six and half years of operation and, since the end of 1964, has been working on a round-the clock basis.

In 1967, particularly during the monsoon months, a series of component breakdowns hindered the smooth running of the Accelerator for long periods. This was attributed to the high humidity in the accelerator and beam rooms. A marked reduction in the relative humidity has since been effected by carrying out modifications in air conditioning system, and during the last six months of the period under report the performance of the accelerator has improved considerably. During these six months --- excluding the month of March 1968, when the annual maintenance work was carried out --- the monthly average machine time utilized for experiments was about 500 hours. Analysis of the machine run and utilization are given separately for (1) January to December 1967 and (2) January to June 1968.

A number of experiments by the various research groups have been completed. These experiments include charged particle induced reactions, particle gamma angular correlation and fast neutron induced fission experiments which are summarised in this report.

ACCELERATOR

I. Analysis of Accelerator Operation:

Machine utilization as a percentage of maximum possible experimental time is given in Fig. 1.

A. 1st January 1967 to 31st December 1967.

Machine run:

1. Total time available from 1st January 1967 .. 31st December 1967	8760 Hours
2. Holiday observed during the period	24 Hours
3. Time used for routine maintenance	624 Hours
4. Major Maintenance work (February - March)	720 Hours
5. Shut down due to non-availability of Liquid Nitrogen 'Dry Ice	812 Hours
6. Time lost due to Chiller and Air Conditioning Plant repairs	72 Hours
7. Shut down due to failure of power and water supply	31 Hours
8. Number of hours accelerator run	2718 Hours
9. Time lost due to breakdowns	3759* Hours
	<hr/>
	8760 Hours
	=====

Machine Utilization (Break up of item No. 8 above)

1. Time utilized for research experiments	1944 Hours
2. Time used for machine conditioning, and repair of beam handling and experimental facilities	774 Hours
	<hr/>
	2718 Hours
	=====

* 840 hours have been spent in transferring insulating gas and roughing the Accelerator tank.

B. 1st January 1968 to 30th June 1968:

Machine run:

1. Total time available from 1st January 1968 to 30th June 1968	4380 Hours
2. Holiday observed during the period	48 Hours
3. Time used for routine maintenance	312 Hours
4. Major Maintenance work (February - March)	624 Hours
5. Shut down due to non-availability of Liquid Nitrogen/Dry Ice	5 Hours
6. Time lost due to Chiller and Air conditioning Plant repairs	71 Hours
7. Shut down due to failure of power and water supply	48 Hours
8. No. of hours accelerator run	2755 Hours
9. Time loss due to breakdowns	51.7* Hours
	<hr/>
	4380 Hours
	=====

Machine Utilization (Break-up of item No. 8 above)

1. Time utilized for research experiments	2311 Hours
2. Time used for testing laboratory moulded belt spacers	48 Hours
3. Time used for acceleration on heavy ions ($^{16}\text{N}^{++++}$)	143 Hours
4. Time used for checking machine calibration	96 Hours
5. Time used for machine conditioning and repair of beam handling devices and experimental facilities	157 Hours
	<hr/>
	2755 Hours
	=====

* 154 hours have been spent in transferring insulating gas and roughing the Accelerator tank

II. Modifications and additions:

1. All the selsyn motors operating the control cords have been replaced with reversible D.C. motors incorporating limit switch and indicating lamps.
2. A liquid nitrogen trap has been fabricated and installed between the main diffusion pump and the booster pump in the accelerator system.
3. Another pair of quadrupole focusing lenses have been fabricated and installed in the beam port. Quadrupole focusing lenses are now used in all the three ports after the switching magnet.
4. The beam centering power supply has been modified for remote operation from the Accelerator control console. A reversible motor has been used for rotating the position selector switch with an indicating lamp at the remote control panel.

III. Accelerator Components:

Some of the accelerator replacement components like Ion sources, Thermo-mechanical leaks etc. are fabricated in the laboratory¹⁾. The re-processed ion source bottles have continued to give excellent service. In a recent modification, a step has been cut out at the beam entry point in the aluminium canal used in the ion source bottle. One such modified ion source bottle has been installed in the accelerator after bench test and it is giving satisfactory service. This source bottle has already completed 1317 hours of operation and is expected to give a much longer service as the possibility of disintegration of the canal at the beam entry point is minimised.

Belt spacers have been fabricated from indigenous material. A few pieces have been moulded from a mixture of silicon dioxide and marble powder using araldite as the binding medium. Four pieces were tested under actual working conditions and found to be satisfactory. These are now installed in place of the original belt spacers. More such belt spacers are under fabrication.

- 1) Van de Graaff Progress Report, T.P. David, B.A.R.C. 291 (1967).

IV. Accelerator breakdowns and repairs:

A series of breakdowns put the accelerator inoperative for long periods mainly during the first half of 1967. Conditions, however, improved towards the end of the year and the machine has been since operating satisfactorily. Some of the major defects developed and rectified are listed below:

1. One charging belt had to be renewed due to wear and tear. The new belt under operation dislodged and broke a belt spacer which in turn damaged the belt and a couple of other belt spacers.
2. The belt absorbed a considerable amount of moisture due to the abnormally high humidity in the room and could not carry up-charge. It took a few days for the belt to give up moisture and carry normal charge.
3. A few combs of the spray bar were damaged. The entire set of charging points were renewed.
4. A total of 7 coils on the terminal alternators were burnt out. The coils were rewound and replaced.
5. Heater coil in the gas dryer unit was burnt out and had to be renewed before putting it into operation.

6. One of the alternator pulley bearings was found worn out. A new bearing was fitted.

7. A number of belt spacers developed minor cracks. The cracks were filled with araldite and the spacers have been put into operation.

Some of the other components which had to be repaired or renewed during this period due to breakdown are the following:

1. High voltage transformer in the belt charge supply unit.
2. Isolation transformer in the Accelerator terminal
3. High voltage bushing on the terminal plate
4. Corona collector point
5. Regatron power supply unit in the analysing magnet stabilizer system
6. Series resistor in the 80 KV focus supply
7. Balance amplifier unit
8. Switching magnet current control unit

V. Acceleration of Heavy Ions:

Oxygen was introduced in the ion source bottle in an attempt to accelerate $2+$ and $4+$ ^{16}O particles. It was found that oxidization of Hg vapour impeded the operation of the diffusion pumps even when the gas feed rate was kept at a possible minimum.

Nitrogen gas was ionized in the source bottle and $^{14}\text{N}^{4+}$ particles could be accelerated and analyzed. Data with these particles bombarding Au and Al targets have been recorded at different energies and detector angles. The spectra have been analyzed and nitrogen peaks identified. Research experiments to be carried out using this beam are under consideration.

VI. Machine calibration:

${}^7\text{Li}(p,n){}^7\text{Be}$, ${}^{65}\text{Cu}(p,n){}^{65}\text{Zn}$ and ${}^{19}\text{F}(p,n){}^{19}\text{Ne}$ reactions were carried out to determine the change, if any, in the K value originally determined. The K value at present was found to be 0.00742 (earlier value : 0.00740)¹⁾.

- 1) 5.5 Million volt Van de Graaff Accelerator at Trombay, A.S. Divatia et al., A.E.E.T/NP/5(1962).

VII. Development Projects:

1. Five Port Switching Magnet¹⁾ :- T.P. David, N. Sarma, M.S. Bhatia and P.R. Sunder Rao - The magnet and power supplies have been assembled and laboratory tests have been carried out. The current stability of the main magnet coil supply has been measured to be $\sim .08\%$. The stabilized low current (0 - 1A) reversible supply for the auxiliary coil has also been built and tested.

Magnet field measurements at various points in the pole gap have been made with a rotating coil null detector type gauss meter. Very good field uniformity has been recorded along planes perpendicular to the beam axis while there is $\sim 1\%$ variation in the flux density along the beam axis at 16,000 gauss as the measuring probe is moved from the centre to the opposite extremes of the pole face.

The 5 - port aluminium switching chamber has been fabricated and tested for high vacuum. All the control slits have been assembled and tested. The magnet has been kept ready for installation.

The quadrupole lenses and vacuum systems required for all the five ports are under fabrication and are expected to be ready in a couple of months when the magnet is planned to be installed replacing the present

3-port switching magnet.

1) Van de Graaff Laboratory Progress Report - T.P. David, B.A.R.C.
291 (1967):

2. Two-way 90° Energy Analyzing Magnet:- T.P. David - It is proposed to build a beam analyzing magnet capable of bending the beam by 90° with exit ports on opposite sides. This is to replace the existing analyzing magnet making it possible to set up experiments also at the entrance side of the beam room now left unused for experimental purposes.

The design work of the magnet yoke, pole pieces and coils has been taken up. The magnet yoke and pole pieces are to be fabricated from Tata 'A' Grade steel which is found to have very satisfactory magnetic properties. The magnet coil is to be wound in sections from electrical grade aluminium tubing of square section joined end to end by argon-arc welding. Cooling water will be passed through these tubes to achieve maximum cooling efficiency. The transistor stabilized magnet power supply will be similar to that of the 5-port switching magnet.

RESEARCH EXPERIMENTS

1. Absolute Total Cross Section for the Reaction $^{51}\text{V}(p,n)^{51}\text{Cr}$ over the Isobaric Analogue Resonance near 2.340 MeV: M.K. Mehta and K.K. Sekharan -

As a continuation of our study of the $^{51}\text{V}(p,n)^{51}\text{Cr}$ reaction¹⁾ utilising a 4π geometry neutron counter²⁾, the absolute cross section has been measured for this reaction in the incident energy range 2.180 to 2.750 MeV. Figure 2 shows the excitation function. There are a large number of peaks in this range. The high intensity peak at 2.340 MeV is the previously identified isobaric analogue resonance³⁾. The dash dot line is considered as the back ground and represents our earlier measurement of the cross section with a 45 KeV target from which the contribution of the analogue resonance is excluded. The cross section was measured in very fine steps (1.25 to 5 KeV) over the resonance near the proton bombarding energy 2.340 MeV. Figure 3 shows the shape of the resonance determined in this experiment. The data-points represent three separate measurements (represented by open and closed circles and crosses) of the excitation function over the resonance with frequent repetitions at a number of energies. The target used was prepared by evaporating vanadium metal on thin carbon backing. The number of ^{51}V atoms present was determined by measuring the elastically scattered alpha particle yield from this target at $E_{\alpha} = 2.0$ and 3.0 MeV and fitting the Rutherford cross section expression to the angular distribution. The target thickness was measured to be $16 \pm 1 \mu\text{gm}/\text{cm}^2$ (~ 1 KeV for 2 MeV protons). An overall absolute error of $\pm 13\%$ and a relative error of $\pm 7\%$ (estimated from the scatter of the points) are assigned to the data points.

This resonance has been shown to be formed by $l = 1$ protons giving

a 4^+ level in ^{52}Cr at 12.8 MeV excitation identified³⁾ as the analogue of the 4^+ level at 1.55 MeV in ^{52}V .

Generally the proton partial width Γ_p and the spreading width W^e for an isobaric analogue resonance are determined from the shape analysis of the (p,p) or (p,p') data. These then lead to the determination of the proton spectroscopic factor and the strength of the mixing between the isobaric analogue state ($T_>$) with the $T_<$ normal states in the compound nucleus. In the present case this resonance occurs as a barely discernible anomaly in the elastic scattering results³⁾ and hence it is not possible to determine any meaningful parameters from that. The inelastic yield would also be negligible⁴⁾ at this energy. Thus the detailed shape analysis of the resonance observed in the (p,n) channel (forbidden for an isobaric state if there is no T mixing) offers the only method to determine the parameters pertinent to the isobaric analogue resonance theory. Accurate and fine resolution measurement of the cross section is essential for such an analysis. In the figure the dash-dot line marked as $\sigma_{p,n}^{\text{total}}(\text{bkg})$ is considered as the background and represents an earlier measurement¹⁾ of the cross section with a 45 KeV target from which the contribution of the analogue resonance is not included. A number of trial fits were made based on the expression given by C.H. Johnson et al⁵⁾

$$\sigma_{pn}(\text{res}) = \sigma_{p,n}(\text{bkg}) \left[\frac{(E - E_0 + \Delta)^2}{(E - E_0)^2 + (\frac{\Gamma}{2})^2} - 1 \right]$$

with E_0 , Γ , Δ and $\sigma_{p,n}(\text{bkg})$ as four adjustable parameters. The solid line is a fit with $E_0 = 2.338 \text{ MeV}$, $\Gamma = 6 \text{ KeV}$, $\Delta = -30 \text{ KeV}$ and

$\sigma_{p,n}(\text{bkg}) = 0.53 \text{ mb}$. Taranishi and Furubayashi⁶⁾ have considered the smaller peaks on the higher energy side (around $E_p = 2.350 \text{ MeV}$) also as a

part of the analogue resonance. If such is the case, it is not possible to find a consistent set of parameters which gives a reasonable fit. The dashed line indicates a fit of such type where a positive value of Δ has to be used to get the 'high energy tail'. The parameters for this fit are $E_0 = 2.338$ MeV, $\Gamma = 8$ KeV, $\Delta = 40$ KeV and $\sigma_{p,n}(\text{bkg}) = 0.535$ mb. The difficulty encountered in the second type of fit coupled with the goodness of the first fit leads to the inference that the peaks on the higher energy side ($\sim E_p = 2.350$ MeV) represent separate structure and not the finer structure of the analogue resonance. An extensive measurement of the excitation curve has been made in fine steps extending over a wider range of energy which shows the presence of a number of such peaks as well as smaller "fluctuations"¹⁾.

A search for the best set of resonance parameters to fit the shape and determination of the analogue state parameters Γ_p and W^e is now underway.

- 1) K.K. Sekharan, M.K. Nehta and A.S. Divatia
Bull. Am. Phys. Soc. 12, (1967) 11 and to be published.
- 2) K.K. Sekharan, A.S. Divatia, M.K. Mehta, S.S. Kerekatte and K.B. Nambiar
Phys. Rev. 156, (1967) 1187.
- 3) J.J. Egan, F. Gabbard, G.C. Dutta, D.E. Barnes and T. Young
Bull. Am. Phys. Soc. 11 (1966) 840 and private communication.
- 4) C.M. Lamba, N. Sarma, N.S. Thampi, S.K. Sood and V.K. Deshpande
Nucl. Phys. A110 (1968) 111.
- 5) C.H. Johnson, R.L. Kernell and J. Ramavataram
Nucl. Phys. A107 (1968) 21.
- 6) E. Teranishi and B. Furubayashi
Proc. of the Conference on Isobaric Spin in Nucl. Phys., Tallahassee, Florida (1966) p. 640.

2. Analysis of Excitation Functions for the $^{27}\text{Al}(p, \alpha_0)^{24}\text{Mg}$ and $^{27}\text{Al}(p, \alpha_1)^{24}\text{Mg}^*$ Reactions: M.K. Mehta and A.S. Divatia - As a continuation of the programme of studying the reactions induced by proton bombardment of aluminium¹⁾, the excitation functions for the reactions $^{27}\text{Al}(p, \alpha_0)^{24}\text{Mg}$ and $^{27}\text{Al}(p, \alpha_1)^{24}\text{Mg}^*$ have been measured at three laboratory angles of 60° , 90° and 165° . The aim of the experiment was to study the correlations between the structures observed in the two alpha channels. The excitation function for the α_0 group at 90° was also one of the excitation functions measured in the previous experiments¹⁾ which was reported at the Calcutta (1965) and the Bombay (1966) Symposia. The experimental details were the same as before. The six excitation functions were measured in steps of 5 KeV with a resolution better than 5 KeV, in the bombarding energy range from 4 to 5.5 MeV and are shown in Fig. 4. As before the curves show fine structure (~ 20 KeV) superimposed on wider structure (100 - 300 KeV). As the $90^\circ \alpha_0$ group curve is a very good reproduction of the previous curve, it is assumed that as before the autocorrelation analysis would, result in Lorentzian fits with $\langle \Gamma \rangle \approx 20$ KeV for small ϵ . This would mean that the narrow structure (~ 20 KeV) represents the effects of the 'compound nuclear' levels in the sense that they have multinucleon character in terms of the statistical model.

The presence of the broader structure can be easily seen in Figs. 5 and 6 which show the excitation curves for the α_0 group at 60° and α_1 group at 90° , respectively. In these figures the lowest curves show the data points as measured with a resolution of less than 5 KeV. This data are then averaged of various intervals δ and the curves obtained for

$\delta = 20, 50, 100$ and 300 KeV are shown in each figure. The narrow structure observed in the $\delta < 5$ KeV curve is completely washed out in the $\delta = 20$ KeV curve where typical structure with Γ_s of about 75, 100, 150 and 200 KeV are indicated. These structures themselves get averaged out with each increasing δ and ultimately for $\delta = 300$ KeV no significant structure is left except for possible (~ 1 MeV wide) bump.

Labelling the curves for α_0 groups at 60° , 90° and 120° as curves A, B and C respectively and the corresponding curves for the α_1 groups as the curves D, E and F respectively, the angular cross correlation $C_{AB}(0)$, $C_{AC}(0)$, $C_{DF}(0)$, $C_{DE}(0)$ as well as the channel cross correlations $C_{AD}(0)$, $C_{BE}(0)$ and $C_{CF}(0)$ were calculated in the notation of reference ¹⁾, using a moving average with the averaging interval δ varying between 50 and 1500 KeV. The results are shown in Fig. 7. It was shown in the previous work ¹⁾ that the significant δ is around 300-400 KeV for which all cross correlation have high values. The angular cross correlations go through a maximum around $\delta = 200$ -300 KeV and then drop very slowly almost flattening out. The channel cross correlations show peaks around $\delta = 300 - 400$ KeV and a minimum around $\delta = 600$ KeV.

Fig. 8 shows the superimposition of the α_0 and α_1 curves which are averaged over 20 KeV for each angle. In this the cross correlation between broader peaks can be seen quite easily. Occasionally a peak in the α_0 curve is missing in the α_1 curve and vice versa. The strong cross correlation exhibited by these peaks would indicate that they represent individual levels in the compound system of the 28 nucleons. The occasionally missing correlation then can be understood as the effect of the angular momentum of the compound state in relation to the spin and parity values of

0^+ and 2^+ of the ground and the first excited states of ^{24}Mg respectively.

The conclusion that can be drawn from this correlation analysis, coupled with the fact that the finer structure is due to the compound nuclear levels, is the following: The wider structures having width $\Gamma \geq 50$ KeV are strongly correlated in the channels as well as in angles for angles greater than the 'coherence' angles. The strong correlations put them in the category of resonances and the observed widths put them into the category of 'intermediate structure'. These intermediate resonances represent excitation energy shared between only a few nucleons in the compound system of $A = 28$ nucleons as against the concept of the 'compound nucleus' which assumes the excitation energy to be completely distributed over the $A = 28$ nucleons. Izumo²⁾ has worked out a theory called the "partial equilibrium model" for such intermediate resonances. He has calculated the position of such resonances in $A = 28$ system assuming that only six nucleons share the excitation. Such resonances would have widths of 100 - 200 KeV. From the data available to him he identifies two levels in the region of excitation between 15.3 and 16.8 MeV, (the region covered by the present experiment). These two are seen in our curves at E_α around 4.10 and 5.00 MeV at excitations of about 15.4 and 16.35 MeV.

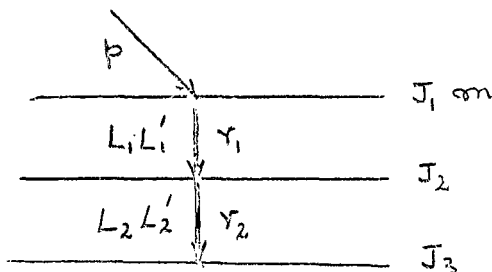
- 1) M.K. Mehta, Joseph John, S.S. Kerekatte and A.S. Divatia
Nucl. Phys. 89 (1966) 22.
M.K. Mehta and A.S. Divatia, Proc. Nucl. Phys. & Sol. State Phys. Symp., India (1966) 80.
- 2) K. Izumo, Nucl. Phys. 62 (1965) 673.
3. Reactions Induced by Alpha Particle Bombardment of ^{19}F : M. Balakrishnan, S.S. Kerekatte, M.K. Mehta and A.S. Divatia - Thin targets, prepared by evaporation of LiF on thin carbon backings, have been bombarded by 3 and 4 MeV

alpha particles. The reaction products are detected by solid state counters placed at various angles with respect to the beam. The α_0 group and the p_0 group, resulting from the reactions $^{19}\text{F}(\alpha, \alpha_0)^{19}\text{F}$ and $^{19}\text{F}(\alpha, p_0)^{22}\text{Na}$ respectively, have been identified in a preliminary analysis of the charged particle spectra obtained in these runs. It is planned to measure excitation functions and the angular distributions for the yield of α_0 and p_0 as well as other identifiable reaction products in the bombarding range from 2 to 5.5 MeV.

4. Computer Programme for the Analysis of 'Collinear Geometry Particle-Gamma Ray Angular Correlations' Measurements in Nuclear Reactions:

M.A. Eswaran - A programme SIMCOR was written in Fortran for the CDC - 3600 computer of TIFR following the method described in the earlier report¹⁾.

The additional feature of this programme is that it is extended to include cases where there will be more than one gamma ray in coincidence with the particle group feeding a particular excited state in the residual nucleus in the nuclear reaction such as $^{29}\text{Si}(d, p \gamma_1 \gamma_2)^{29}\text{Si}$ as shown in the figure.



In such a case the angular correlation expression for $p - \gamma_1$ is²⁾

$$W(\theta_1) = \sum_{m, L_1, L_1'} P(m) \delta_1^{L_1} \sum_K C_{k_0}^0 (J_1 J_2 L_1 L_1' m) Q_k \bar{P}_k (\cos \theta)$$

and for p - γ_2 correlation where γ_1 is an unobserved intermediate radiation,

$$W(\theta_2) = \sum_{L_1 L_1' L_2 L_2'} P(m) \delta_1^{p_1} \delta_2^{p_2} \sum_M C_{OM}^0 (J_1 J_2 J_3 L_1 L_1' L_2 L_2' m) Q_M P_M (\cos \theta)$$

When both correlations are measured simultaneously say at 7 angles, then there are 7 data points due to p - γ_1 , correlation and 7 more data points for p - γ_2 correlation. However all the 14 equations corresponding to 14 data points involve the same unknowns P(m), the population parameters for the magnetic substates.

In the programme least squares fit analysis is done taking the data points of both the correlations simultaneously and whole range of δ_1 and δ_2 , the quadrupole to dipole amplitude mixing ratios of γ_1 and γ_2 are covered to obtain series of χ^2 values. Finite particle counter size effect is also included by providing for introduction of contribution from higher magnetic substate. This programme has been used in the case of study of 3.067 MeV from the excited state in ^{29}Si which decays by cascade through 1.277 MeV first excited state. This is described in the next article.

- 1) Van de Graaff Laboratory Progress Report BARC-291 (1967) and M.A. Eswaran, N.L. Ragoowansi and P.C. Mitra BARC Report 276 (1967).
- 2) P.B. Smith in 'Nuclear Reactions' Vol. II, North Holland Publ. Co., Amsterdam.

5. Proton-Gamma Ray Angular Correlation Studies in the Reaction $^{28}\text{Si}(d, p)^{29}\text{Si}$

M.A. Eswaran, M. Ismail, N.L. Ragoowansi and P.C. Mitra - Spins of the ^{29}Si

excited states at 1.277 -, 2.027 - and 2.425 MeV excitation energy have been well established¹⁾; however, for the 3.067 MeV fourth excited state spin is not uniquely assigned. In the present work proton-gamma ray angular correlation measurements were made in the reaction $^{28}\text{Si}(d,p\gamma)^{29}\text{Si}$ for the study of first four excited states, in collinear geometry detecting protons at 0° to the beam, employing the analysis procedure, which is independent of any assumption regarding reaction mechanism.

A 99% isotopically enriched ^{28}Si target (supplied by A.E.R.E., Harwell) of thickness $\sim 100 \mu\text{g}/\text{cm}^2$ on tantalum backing was bombarded by deuteron beam in the energy range 2.50 to 3.10 MeV and the outgoing protons were detected in a 600 μm thick ORTEC surface barrier detector at zero degree subtending a half-angle of 5° at the target, the deuteron beam being stopped by sufficient tantalum foils placed at the back of the target. Gamma rays were detected in 12.7 cm.dia. x 15.2 cm. long NaI(Tl) scintillation detector and the γ -ray spectrum was recorded in one half of 400 channel pulse-height analyser in coincidence with the selected group of proton pulses from the particle detector using a conventional fast-slow coincidence arrangement of resolving time $2\tau = 4 \times 10^{-9}$ sec. Random coincidence spectrum was recorded simultaneously in the other half of the 400 channel pulse-height analyser using the pulses due to ground state group of protons p_0 selected in a 20 channel pulse height analyser in the slow side of the fast-slow gating system. Such coincidence spectra were recorded at 7 angles from 0° to 90° in steps of 15° for the position of the gamma detector with respect to the beam axis, successively selecting p_1, p_2, p_3 and p_4 proton groups feeding the first four excited states in ^{29}Si in the gating system. The main difficulty in these experiments is the large neutron background which

activates the NaI in the gamma detector giving rise to high background counting rate in the detector due to ^{128}I and ^{24}Na activities. This was minimised by using borated paraffin and boron carbide shields in front of the gamma detector.

Fig. 9 shows the gamma ray spectra recorded in coincidence with the proton groups p_1 , p_2 and p_3 feeding the first, second and third excited state, using deuteron beam energies (E_d) of 2.60, 2.50 and 2.75 MeV respectively. Spectra shown are the sum of the 7 spectra taken at various angles for each excited state. Fig. 10 shows the gamma ray spectra recorded in coincidence with the proton group p_4 feeding the fourth excited state. Angular correlation data deduced from these measurements are shown in Figs. 11 and 12. For obtaining these, photo-peak counts were used and correction due to Compton contribution of higher energy gamma rays whenever necessary and absorption correction due to proton counter situated at 0° etc. have been applied.

A computer programme for CDC-3600 was written for analysis of these data using the method II of Litherland and Ferguson²⁾. The details of the analysis in terms of the linear least squares fitting procedure treating the magnetic substate population parameters as unknowns has been described in the earlier article. From the χ^2 analysis spin value of 3/2 could be assigned for the 1.277 - and 2.425 MeV first and third excited states ruling out 5/2. For the 2.027 second excited state both 3/2 and 5/2 spin choices fit the correlation data.

In the case of 3.067 MeV fourth excited state the predominant mode of decay (80%) is through the 1.277 MeV first excited state. Both the

angular correlations of $P_4 - \gamma_{1.79}$ ($3.067 \rightarrow 1.277$ MeV) and $P_4 - \gamma_{1.277}$ ($1.277 \rightarrow 0$ with 1.79 MeV γ -ray unobserved) are shown in Fig. 12. Provision was made in the computer programme to treat the data of both these angular correlations simultaneously. From this χ^2 analysis spin of 7/2 can be ruled out for the 3.067 MeV state. Both 3/2 and 5/2 choices for the spin of this state give equally good fits.

- 1) P.M. Endt and C. Van der Leun
Nucl. Phys. A105 (1967) 1
- 2) A.E. Litherland and A.J. Ferguson
Can. J. Phys. 39 (1961) 788

6. Spin and Parity Assignment to the Level at 14.378 MeV in ^{28}Si :

S.S. Kerekatte, M. Balakrishanan, M.K. Mehta and A.S. Divatia - In the elastic scattering of alpha particles by ^{24}Mg , seven resonances, corresponding to levels in the compound nucleus ^{27}Si , were observed in the excitation function¹⁾. Out of these seven resonances, the one at 14.378 MeV excitation corresponding to $E_\alpha = 5.126$ MeV, was selected for analysis, because it is narrow and also to see whether single level analysis can be applied at high excitations.

The data on this resonance existed at four selected centre-of-mass angles: 90° , 125.3° , 149.5° and 166.6° . From the vanishing of the resonance at 149.5° (at which angle $P_4(\cos\theta) = 0$), a tentative assignment of $J = 4^+$ was made to this level¹⁾.

The data at these four angles, were analysed on the CDC - 3600 computer. A Fortran programme was written, based on the single level dispersion expression, for the differential elastic scattering cross-section, given by Blatt and Biedenharn²⁾. The programme was originally written for

the analysis of the ${}^6\text{Li}(\alpha, \alpha){}^6\text{Li}$ data³⁾. However, the expression simplifies considerably due to the fact that in the scattering of zero-spin particles (alphas) by a zero-spin nucleus (${}^{24}\text{Mg}$), the angular momentum of the partial wave involved, is directly equal to the spin of the state excited in the compound nucleus (${}^{28}\text{Si}$ in this case).

The resonance shapes which are possible for a J^{π} value of 4^+ , were calculated on the computer, using the above-mentioned Fortran programme. A channel radius of 5.8 fermis was used in this calculation. The calculated shapes have been compared with the experimental data, after suitable normalization (Fig. 13). The smooth curves are the calculated shapes, while the points (with the error magnitudes marked on them), represent the experimental data. The fits are extremely good, except for small deviations away from resonance, thus confirming the spin and parity assignment. The deviations represent the contributions from the neighbouring levels, which have not been taken into account. The good fits of the data show that single level analysis can be applied even at excitations in the region of 14 MeV. Since, the data has not been reduced to absolute cross-sections, the determination of other resonance parameters such as the total width, the reduced width, the phase shift, etc., was not attempted. The Wigner limit in the present case, ${}^{24}\text{Mg} + \alpha$, considering the alpha as a single particle, is 544 KeV for an interaction radius of 5.8 fermis. We believe that the observed width of about 5 KeV, has a considerable fraction due to the target thickness which is estimated to be about 4 KeV. Thus, the natural width of the level would be about 3 KeV. A 4^+ state having a reduced width equal to the Wigner limit (544 KeV) would have an experiment-

al width of 24 KeV, using the expression $\Gamma_{\text{experimental}} (\ell = 4, J = 4) =$

$$2P\gamma^2 \text{ where } \gamma^2 = \frac{5}{2} \frac{\hbar^2}{\mu a^2},$$

$$P = \left[\frac{K\gamma}{F_\ell^2 + G_\ell^2} \right]_{r=a}$$

This makes the actually observed width about 12% of the width expected from the Wigner limit. The conclusion is that single level analysis can be applied even at high excitations ~ 14 MeV.

- 1) S.S. Kerekatte, et al, Proc. Nucl. Phys & Sol. State Phys. Symp., India (1967) 158.
- 2) J.M. Blatt and L.C. Biedenharn, Revs. Modern Phys. 24, (1952) 258
- 3) M. Balakrishnan et al, Proc. Nucl. Phys. & Sol. State Phys. Symp., India (1968).

7. Study of the Reactions $^{19}\text{F}(p, \alpha_0)^{16}\text{O}$ and $^{19}\text{F}(p, \alpha_{1+2})^{16}\text{O}$: K.V.K. Iyengar*, B. Lal*, M.K. Mehta, K.K. Sekharan and M.Y. Vaze - The yields of α_0 groups in the reaction $^{19}\text{F}(p, \alpha)^{16}\text{O}$ were measured to locate resonances in the compound nucleus ^{20}Ne and to search for structures wider than the usual compound nucleus resonances. The excitation functions for the α_0 's going to the ground state of ^{16}O at the lab. angles of 90° and 120° and the (unresolved) α_{1+2} 's going to the first and second excited states of ^{16}O at the lab angles of 90° , 120° and 165° were measured in the incident proton energy range 2.000 - 3.625 MeV in steps of 25 KeV. The excitation function of the α_0 group at 165° could not be measured with any reliability as the yield at 165° is very low.

The proton beam from the Trombay 5.5 MeV van de Graaff was used to bombard a thin CaF_2 target evaporated on thin carbon backing. A typical

* Tata Institute of Fundamental Research, Bombay.

spectrum of reaction products for $E_p = 3.175$ MeV at the lab angle of 120° is presented in Fig. 14. The excitation functions are presented in Fig. 15. A large number of peaks are seen in all the excitation functions. The cross correlation between excitation functions of the same group at different angles are calculated. As expected the curves 2 and 4 corresponding to α_0 group at the lab angles 90° and 120° and curves 1 and 3 corresponding to α_{1+2} group at the lab angles of 90° and 120° are correlated (the coherence angle being 36°) and the calculated values are 0.46 and 0.67 respectively. In addition to these, we find that the curves 1 and 5 corresponding to α_{1+2} group at the lab angles of 90° and 165° are also correlated and the value is 0.57. The cross correlation between 3 and 5 corresponding to α_{1+2} group at the lab angles of 120° and 165° is found to be 0.56.

As is obvious from Fig. 15 there does not exist much of correlation between the different groups at the same angle which is perhaps due to the fact that the compound nucleus levels preferentially decay either to the ground state or to the second excited state as the spins of the two states are quite different. The spins and parities of the ground state, 1st and 2nd excited states of ^{16}O are 0^+ , 0^+ and 3^- respectively. The cross correlation between α_0 and α_{1+2} groups where observed, is likely to be due to the correlations between α_0 and α_1 groups.

The mean width of levels of the compound nucleus of ^{20}Ne at the excitation energies under investigation is expected to be around 65 KeV on statistical model considerations¹⁾ whereas many of the peaks seen in the excitation functions are of width less than 100 KeV implying that the

structure seen in the excitation functions represent resonances arising from the excitation of levels of the compound nucleus ^{20}Ne . Levels in ^{20}Ne at excitation energies as high as 15 MeV have been identified²⁾ as members of rotational bands in ^{20}Ne . It is therefore proposed to study the angular distribution of the α 's to the ground state of ^{16}O by direct observation of the alphas and those to the first and second excited states of ^{16}O by α - γ coincidences at the resonance energies to determine the spin and parity of the corresponding levels in ^{20}Ne . These studies may help in the identification of additional members of these bands. Arrows marked in the excitation curves shown in Fig. 15 represent the resonances which have already been observed²⁾ in $^{16}\text{O}(\alpha, \alpha)$ yield studies.

When excitation curves are averaged over 100 to 300 KeV some wide peaks are also observed. The original and the averaged excitation functions are presented in Fig. 16. The wide peaks can be interpreted in terms of intermediate resonances described by the partial equilibrium model of Izumo³⁾ as arising from the excitation of a few nucleons outside an inert core. There is a wide resonance with a peak around $E_p = 2.6$ MeV which is observed in all the excitation functions of the α_{1+2} group. This corresponds to an excitation energy of 15.2 MeV in ^{20}Ne . This is in good agreement with an intermediate resonance of similar width predicted by Izumo at an excitation energy of 12.2 MeV for a system of 28 nucleons, when the number of active nucleons is 6. In addition we see a resonance at an excitation energy of about 15.8 MeV in ^{20}Ne corresponding to an incident proton energy of 3.1 MeV and of width

about 600 KeV which is larger than the widths of intermediate resonances predicted by Izumo. If this is due to an intermediate resonance it is then likely that the number of active nucleons responsible for it is less than six.

- 1) T. Ericson and T. Mayer-Kuckuk, Ann. Revs. Nucl. Sci. 16 (1966)
- 2) M.K. Mehta, W.E. Hunt and R.H. Davis, Phys. Rev. 160 (1967) 791 and W.E. Hunt, M.K. Mehta and R.H. Davis, Phys. Rev. 160 (1967) 782.
- 3) K. Izumo, Nucl. Phys. 62 (1965) 673.

Presented at the Nucl. Phys. and Solid State Phys. Symp. India (1968)

8. Intermediate Structure in $^{19}\text{F}(d, n)^{17}\text{O}$ Reaction: M.G. Betigeri, C.M. Lamba, N. Sarma and D.K. Sood* - According to the concept introduced by Feshbach¹⁾, the intermediate states are believed to have modes of excitation whose complexity lies between the complicated compound nuclear state and that of single particle state. It, therefore, follows that while compound nuclear states involve complete statistical equilibrium and single particle states involve only one particle, an intermediate state should arise from a partial equilibrium of the incoming particle of n nucleons with only a few (N) nucleons outside an inert core²⁾. Starting from this point, Izumo has calculated the level spacings from $N + n = 5, 6$ and 7 treating $(N + n)$ nucleons as a Fermi-gas with ξ - interaction. It is evident that so long as the number of nucleons $(N + n)$ outside the core is the same, the various properties of the intermediate states such as spin, parity, width and spacing should remain the same irrespective of the reaction through which the states in question are formed. For a Fermi gas, the dependence of excitation energies E of the resonances on the

* Indian Institute of Technology, Kanpur, India.

the nuclear radius R characteristic of (A + n) system is given by

$$ER^2 = \text{constant}$$

When the same number of outer nucleons are excited, the same intermediate resonances will appear in all compound nuclei at excitation energies related by the above relation. Izumo³⁾ has collected a large number of excitation functions and has found that most of the experimental data on intermediate states can be put in 3 classes with (n + N) = 5, 6 and 7.

Assuming a configuration of $^{16}\text{O} + 5$ nucleons for ^{21}Ne , the expected positions of resonances calculated from this model are shown in the Table given below:

Resonances observed in $^{19}\text{F} + d$ channel compared
with the predicted ones for n + N = 5 and 6

No.	Resonance Energies in ^{21}Ne (MeV)				
	Experimental			Theoretical	
	Present data	$^{19}\text{F}(d,n)^{6,7)}$	$^{19}\text{F}(d,p)^4)$	N + n = 5	N + n = 6
1	1.65	1.47	1.65	1.521	1.495
2	2.15	2.17	2.15	2.073	-
3	2.70	-	-	2.801	2.624
4	3.25	3.20	-	3.338	3.292
5	3.75	3.80	-	3.900	4.087
6	4.55	4.2	-	4.599	4.356
7	5.10	-	-	5.265	4.947

The available data on $^{19}\text{F}(d,p)$ and $^{19}\text{F}(d,\alpha)$ reactions^{4,5)} showed resonances at $E_d = 1.521$ MeV and $E_d = 2.073$ MeV, in conformity with the expected position of resonances. It was, therefore, of interest to extend the data to higher energies.

We report measurements on the excitation function for $^{19}\text{F}(d,\alpha)^{17}\text{O}$ reaction from 2 MeV to 5.2 MeV. The excitation functions for α_0 ($\theta_{\text{lab}} = 94.2^\circ$) and α_1 and α_2 ($\theta_{\text{lab}} = 150^\circ$) are plotted in Fig. 17. The present work reproduces the earlier data between 2 MeV and 2.5 MeV. Resonances are observed at incident deuteron energies $E_d = 2.15, 2.70, 3.25, 3.75, 4.55$ and 5.10 MeV. The widths of these resonances increase with the excitation energy in ^{21}Ne as expected from the Fermi-gas model.

In Fig. 18 the excitation functions for the reaction $^{19}\text{F}(d,n)^{20}\text{Ne}$ ^{8,7)} and the reaction $^{19}\text{F}(d,p)^{20}\text{F}$ ⁴⁾ are compared with the present data. The resonances found in the present study are also to be seen in the other channels which populate the same state in ^{21}Ne . The positions of the resonances as seen in ($^{19}\text{F} + d$) channel leading to protons, neutrons and α -particles in the outgoing channel are listed in the Table. The agreement with the expected positions for $N + n = 5$ is remarkably good, compared with that of $N + n = 6$, confirming the $^{16}\text{O} + 5$ nucleon configuration for ^{21}Ne even at ~ 20 MeV excitation.

It is surprising that no fluctuations of the Ericson type are observed at these excitation energies (18 - 23 MeV). A study of $^{23}\text{Na}(d,\alpha)^{21}\text{Ne}$ reaction⁸⁾ also indicates the absence of Ericson fluctuations. Recently⁹⁾ an attempt has been made to analyse the reaction $^{19}\text{F}(d,\alpha)^{17}\text{O}$ in terms of fluctuations. It is hard to justify this analysis in view of the small

sample size (6 resonances in 3.2 MeV region), coupled with the fact that the resonances observed in our study are also seen in (d,p) and (d,n) channels. The experimental data of reference 9, however, between $E_d = 1$ and 4 MeV is in agreement with the present data.

- 1) H. Feshbach, A.K. Kerman and R.H. Lemmer, Ann. Phys. 41 (1967) 230.
- 2) K. Izumo, Prog. Theo. Phys. 26 (1961) 807.
- 3) K. Izumo, Nucl. Phys. 62 (1965) 673.
- 4) A.Z. El Behay, M.A. Farouk, V.J. Gontchav, V.A. Loutsik, M.H. Nassef and I.I. Zaloubovsky, Nucl. Phys. 56 (1964) 224.
- 5) A.Z. El Behay, M.A. Farouk, M.H. Nassef and I.I. Zaloubovsky, Nucl. Phys. 61 (1965) 282.
- 6) S.I. Warshaw, D.A. Goldberg and G.E. Owen, Phys. Rev. 151 (1966) 834.
- 7) A.W. Barrows, F. Gabbard and J.L. Weil, Phys. Rev. 161 (1967) 928.
- 8) R.S. Cox, E.N. Strait and R.A. Fisher, Bull. Am. Phys. Soc. 12 (1967) 913.
- 9) Y. Takeuchi, Y. Hiratate, K. Miura, T. Tohei and S. Morita, Nucl. Phys. 109 (1968) 105.

9. Study of the $^{29}\text{Si}(\alpha, n)^{32}\text{S}$ Reaction from 3.0 to 5.40 MeV: M. Bala-krishnan, K.K. Sekharan, M.K. Mehta and A.S. Divatia - A preliminary run has been made to measure the excitation curve for the reaction $^{29}\text{Si}(\alpha, n)^{32}\text{S}$. The target consists of 84% ^{29}Si (supplied by A.E.R.E. Harwell) on 1/4 mil tantalum backing. The 4π geometry neutron counter described earlier¹⁾ was used to measure the neutron yield. The aim of the experiment is to obtain the absolute cross section for the $^{29}\text{Si}(\alpha, n)^{32}\text{S}$ reactions which can then be used to calculate the cross section of the inverse reaction $^{32}\text{S}(n, \alpha)^{29}\text{Si}$ using the reciprocity relations. The latter cross section has significance in terms of required nuclear data for reactor physics. Beyond 4.4 MeV the

yield will have a contribution due to the n_1 group going to the first excited state of ^{32}S and as the 4π counter does not differentiate between the n_0 and n_1 groups, the reciprocity theorem can not be applied. Figure 19 shows the results of the first run. There is a large amount of structure. The sharp peaks may be due to individual resonances or Ericson fluctuations. The outstanding feature of the curve is the presence of three strong peaks at 4.90, 5.04 and 5.21 MeV bombarding energies.

The Coulomb barrier for the alpha particle on ^{29}Si is about 6 MeV and these peaks are below the barrier. There is a strong probability that even if the other structure represents fluctuations these three peaks are resonances due to individual levels in the compound nucleus ^{33}S . It is planned to measure the excitation function for the 2.4 MeV gamma ray from the first excited state of ^{32}S populated by the n_1 group.

1) K.K. Sekharan, A.S. Divatia, M.K. Mehta, S.S. Kerekatte, and K.B. Nambiar, Phys. Rev. 156 (1967) 1187.

10. Shape Analysis for the 3.5 MeV Resonance Observed in the Alpha Scattering

^6Li : M. Balakrishnan, S.K. Gupta*, M.K. Mehta and K.B. Nambiar - The levels in ^{10}B are important from the following reasons. With mass number ten, this particular nucleus falls in the middle of the 1P shell and hence has the tendency towards collective behaviour. The intermediate-coupling calculations^{1,2)} have been found to be successful for light nuclei in this region, and for a precise testing of its validity, the energy levels and level parameters must be accurately known. An investigation of the elastic scattering of α -particles in ^6Li was under taken³⁾ to study further the level properties of the unassigned levels in ^{10}B . The present work refers to a

* Tata Institute of Fundamental Research, Bombay.

resonance at 3.50 MeV bombarding energy corresponding to an excited level at 6.56 MeV in ^{10}B .

Singly ionized alpha particles were accelerated in the 5.5 MeV van de Graaff generator and were scattered from ^6Li in the energy region $E(\text{lab}) = 3.20$ to 3.80 MeV. We have used 99% enriched ^6Li targets (10 KeV thick) of about $10 \mu\text{gms}/\text{cm}^2$ deposited on very thin self supporting carbon foils of about $5-10 \mu\text{gms}/\text{cm}^2$ thickness. The excitation functions were measured in 10 KeV steps at four different lab angles 43° , 56.3° , 71° and 84° (corresponding to CM angles 70.1° , 90° , 109.8° and 125.3° respectively) around the resonance observed at 3.5 MeV mentioned in our earlier report³⁾. Silicon detectors coupled to low noise pre-amplifiers and amplifier were used to feed the alpha-particle-pulses to a 400 channel analyzer.

Fig. 20d shows the measured shapes. The resonance is found to occur at 3.50 MeV which corresponds to an excitation energy of 6560 KeV in ^{10}B nucleus. At 90° c.m., where all the odd polynomials vanish the resonance is symmetric with full width at half maximum of 43 KeV which corresponds to 26 KeV in c.m. At other angles it shows typical dispersion shapes with interference. The symmetry of the resonance at 90° indicates odd parity for the level, which can be inferred from the single level expression⁴⁾.

The data were analysed using R-matrix formalism, for which a convenient version of the general expression for cross section in elastic channel is given by Blatt and Biedenharn⁴⁾. A Fortran programme was written for this expression after making the necessary phase correction as indicated by Huby⁵⁾. Since in the case of ^6Li the ground state $J^\pi = 1^+$ the incident channel spin is 1 and this complicates the procedure of shape analysis

considerably. The threshold for the 1st inelastic group is 3.64 MeV and that for ${}^9\text{Be} + \text{P}$ channel is 3.59 MeV, one can treat this as a one level on channel case. Assuming a channel radius of 5 fm, the possible resonance shapes at the four c.m. angles were calculated for J^π values, 1^+ , 1^- , 2^+ , 2^- , 3^+ , 3^- and 4^- (Fig. 20).

The width of the level was taken to be 25 KeV(c.m.). The few possible cases are shown in figure 20. $J^\pi = 4^-$ level can be formed by $l = 3$ and 5. $l = 5$ is ruled out from kinematic considerations. $J^\pi = 2^-$ can be formed by $l = 1$ and 3. A 2^- level formed with $l = 1$ gives reasonable agreement in the forward angles; where as $J^\pi = 2^-$, $l = 3$ gives good fit in the backward angles. So different ratios of a mixture of l - values were also tried. The result for the best ratio is given in Fig. 20d.

Our present analysis indicates that the level at 6.56 MeV in ${}^{10}\text{B}$ giving rise to the observed resonance at $E_\alpha = 3.50$ MeV has a spin parity 2^- formed by a mixture of $l = 1$ (25%) and $l = 3$ (75%) waves. Meyer et al ⁶⁾ have analysed in a similar way their data, at six angles two of which are common with our data. They assigned $l = 3$ forming 2^- or 4^- state. But the shape at 70° shows the presence of $l = 1$ wave which they could not infer as they have no measurement at 70° . An absolute value of the cross section will be more useful though in practice it is very difficult with pure ${}^6\text{Li}$ target, since no definite composition can be assumed for the proportion of Li_2O and LiOH present in the target, thereby rendering the weighing of the target useless.

- 1) D. Kurath, Phys. Rev. 101 (1956) 216
D. Kurath Phys. Rev. 106 (1957) 975

- 2) A.N. Boyarkine Izv Akad. Nauk. SSSR. Ser. Fiz. 28, No.2 (1964) 337-58.
- 3) Proc. Nucl. Phys. and Sol. State Phys. Symp. India (1967) 162.
- 4) J.M. Blatt and L.C. Biedenharn, Revs. Mod. Phys. 24, (1952) 258.
- 5) R. Huby Proc. Phys. Soc. (London) 67A (1954) 1103
- 6) V. Meyer, R.E. Pixley and P. Truol, Nucl. Phys. A101 (1967) 321.

11. Angular Anisotropy of Fission Fragments in Ternary Fission of ^{235}U

Induced by 3 MeV Neutrons: D.M. Nadkarni - The values of angular anisotropy of fragments in binary and ternary fission of ^{235}U induced by 3 MeV neutrons have been determined with two independent methods. In the first method fission fragments and long range alpha particles were detected with a gridded ionization chamber and a CsI crystal respectively and in the second method semi-conductor detectors were used to detect fission fragments and long range alpha particles. The values of $\left[\frac{N(0^\circ)}{N(90^\circ)} \right]$ for cases of binary and ternary fissions are found to be different. The probability for emission of long range alpha particles in 3 MeV neutron induced fission is found to be lower than that in thermal neutron induced fission. A decrease in the average single fragment kinetic energy of ternary fragments compared to that of binary fragments is observed in 3 MeV neutron induced fission similar to that in thermal neutron fission. It is shown that on the basis of the angular distribution of long range alpha particles and ternary fragments it is possible to learn at what stage in the fission process the long range alpha particles are emitted.

Published in Nucl. Phys. A112, No. 2 (1968) 241.

12. Mossbauer effect following Coulomb Excitation and Recoil Implantation:

R.P. Sharma*, J.K. Shrivastava* and K.G. Prasad* - Enriched Fe - 57 was

* Tata Institute of Fundamental Research, Bombay.

deposited on copper and bombarded with 3.5 MeV α -particle. Target was cooled at liquid nitrogen temperature. Preliminary data has been obtained and the work is in progress.

13. Inelastic Scattering of Protons and Coulomb Excitation with odd Mass Nb, Rh, Ag, In and Au Nuclei: R.P. Sharma*, K.G. Prasad* and V.R. Pandharipande* - $(p, p' \gamma)$ and $(\alpha, \alpha' \gamma)$ experiments were carried out on Nb, Rh, Ag, In and Au nuclei. The experiment has been completed. The calculations of reduced E2 transition probabilities and excitation function is in progress.

14. Perturbed Angular Correlation Measurements Following Recoil Implantation: M.C. Joshi*, H.G. Devare* and P.N. Tandon* - Coulomb excitation in alloys, specially iron in rare earths, was observed for various energies of α -particles. These were the preparatory experiments for carrying out perturbed angular correlation measurements following the recoil implantation.

15. Inelastic Scattering of Protons with I and Sb Nuclei: H.G. Devare* and P.N. Tandon* - $(p, p' \gamma)$ measurements were carried out in Iodine and Antimony isotopes. The emitted γ -rays were detected in a Ge(Li) detector. Calculations of BE2's and excitation functions are in progress.

16. A Study of ^3He Induced Reactions on ^{12}C : C.M. Lamba, N. Sarma and N.S. Thampi - Reactions $^{12}\text{C}(^3\text{He}, ^3\text{He})$ and $^{12}\text{C}(^3\text{He}, p_1, p_2, p_3, p_5)$ at incident ^3He energy of 5.5 MeV were studied. Previous study of this reaction at this energy has been reported by several authors, but no conclusions could be drawn about the reaction mechanisms and nuclear structure. The

* Tata Institute of Fundamental Research, Bombay.

angular distribution for (^3He , ^3He) measured by Parry et al showed a bulk diffraction structure. This structure was then thought to be the surface fringe effect.

This structure can also creep in from the usual compound nuclear fluctuations. As ^3He is a loosely bound particle it excites the compound nucleus (^{15}O) to a high excitation where the levels overlap. This, gives an idea that perhaps ^{15}O is in a statistical mode. This is confirmed by a recent observation by Blake et al of excitation functions for various (^3He , n) and (^3He , p) groups. They find little correlation between peaks and valleys in the cross section either for one group at different angle or for different groups at same angle.

The angular distribution of ^3He elastic group and 5 outgoing proton groups from energy 5.290 to 5.500 in 10 KeV steps with an overall resolution of about 8 KeV were measured.

The various angular distribution for all the groups showed an irregular behaviour with energy. All the angular distribution for a particular group have been averaged and are shown in Figs. 21 and 22. All the distributions show the direct reaction structure at forward angles. Physically this averaging means that the contribution to measured cross section from direct and compound sources become incoherent.

The shape elastic contribution is evaluated by optical model with the help of code ABACVS-II. The optical potential V is of the form

$$U = V - V \left[1 + \exp\left(\frac{r - r_0}{\lambda r}\right) \right]^{-1} - i W_v \left[1 + \exp\left(\frac{r - r_0 v}{a_i v}\right) \right]^{-1} + W_s \left[\exp\left(-\frac{r - r_0 s}{\lambda s}\right) \right]$$

No account of spin orbit forces have been taken because polarisation data is not available and it's introduction makes little effect on differential cross section.

The compound elastic for (^3He , ^3He) and compound reaction parts of p_1 , p_2 , p_3 and p_5 groups have been calculated according to statistical model. The matrix element for channel C to C' is expressed as

$$\langle |M| \rangle^2 = \frac{T_c^{J\pi} T_{c'}^{J\pi}}{\sum_{c''} T_{c''}}$$

T's denote various transmission coefficients. The denominator, as in all the channels complete information about spin and parities various levels is not known, is replaced by

$$\sum_{c''} T_{c''}^J = 2\pi \frac{\Gamma_J^1}{D_J}$$

$$D_J = D_0 / (2J + 1) \exp(-J(J + 1)/2\sigma^2)$$

Under these approximations the cross section reduces to

$$\left\langle \frac{d\sigma^-}{d\Omega}(\theta) \right\rangle = \frac{\lambda^2}{4(2J + 1)(2i + 1)} \frac{D_0}{2\pi\Gamma^1}$$

$$\sum_{s'l's'l'LJ} \frac{T_c T_{c'} (-1)^{s'-s} \bar{Z}(lJ lJ; sL) * \bar{Z}(l'J l'J; s'L) \times P_L \cos(\theta)}{(2J + 1) \exp(-J(J + 1)/2\sigma^2)}$$

A programme GHERAO has been written to calculate this contribution. As it is clear this contribution contains two important compound nuclear parameters $\frac{\Gamma}{D_0}$ and σ which are known as level overlap and spin cut off parameters.

As is well known lot of ambiguities exist in optical potential. Particularly for ^3He the situation is worst because no systematic trend of potential with A and Energy is available. However all the data can broadly

be classified into two categories. One of shallower potentials¹⁾ and other of deeper potentials²⁾.

We have analysed the data with both types of potentials. To the optical part an addition of compound contribution was made by programme GHERAO which was coupled to ABACUS II. The best fit shallower potentials are shown in Fig. 21a along with the fit. It is to be emphasised that this set is completely different from the earlier available set¹⁾. The deeper potential set given by Bessel et al²⁾ fit in data for large range of nuclei and large energies. We have taken the starting point parameters as in Ref. (2) and the best fit is obtained for the optical and compound parameters which are shown with the fit in Fig. 21b. The parameters are very close to the Bessel parameters. One more interesting point is that the values of $\frac{\Gamma}{D_0}$ and σ obtained by two different potential set is almost the same. This is not surprising because these two potential sets do not give the very different transmission coefficients and as the cross section at backward angles is mostly determined by compound part, the $\frac{\Gamma}{D_0}$ and σ parameters which determine the compound part also remain the same.

The averaged angular distributions for p_1, p_2, p_3, p_5 are shown in Fig. 22. As is clear from Fig. p_1, p_3, p_5 group show lot of direct effect in terms of forward peaking while the p_2 group has averaged almost to a symmetric structure around 90° . The cross section at backward angle is determined in these case mostly by compound part. The transmission coefficients, available for input channel for both the potential sets [fits shown by — (shallow) and ---- (deeper)] have been tried. The best fits for different

groups are shown in Fig. 22. The fit for p_2 group is exact while for p_3 and p_5 have been fitted only at backward angle. It is assumed that the contribution at backward angles is mostly compound in nature. The structure in p_1 compound nuclear group did not permit any fitting.

It is interesting to note that various $\frac{V}{D_0}$ and α values for all the groups and for both the potential match very well with the values obtained from elastic scattering analysis. The average values of $\frac{V}{D_0}$ and α are 2.5 and 1.05 respectively.

1) The Optical model of Elastic Scattering Hodgson (1963) Clarendon Press Oxford.

2) P.E. Hodgson, Proc. Int. Congr. on Nucl. Phys. Vol I (Paris 1964) 257.

17. Yield of Charged Particle Groups from $^{45}\text{Sc}+d$: K.V.K. Iyengar*, B. Lal*, P.J. Bhalerao, M.K. Mehta, K.K. Sekharan - This scandium target evaporated onto a carbon film has been bombarded by deuterons in the energy range 2.00 to 2.80 MeV. Spectra of charged particles originating thus have been recorded in steps of 25 KeV at four laboratory angles 40° , 90° , 149° and 165° using semiconductor surface barrier detectors. The spectra are being analysed to obtain the excitation functions of elastically scattered deuterons and various alpha particle groups leading to the ground state and first few excited states of the residual nucleus.

18. The Angular Distribution of Neutrons from $^{13}\text{C}(\alpha, n)^{16}\text{O}$: B. Lal*

K.V.K. Iyengar* and K.K. Sekharan - Nuclear emulsions were exposed to neutrons from $^{13}\text{C}(\alpha, n)^{16}\text{O}$ reaction to study the spin and parities of the

* Tata Institute of Fundamental Research, Bombay.

levels in the compound nucleus ^{17}O , by measuring the angular distributions of neutrons. For both the $^{13}\text{C} + \alpha$ and $^{16}\text{O} + n$ the channel spin is $1/2$ with parities $(-1)^{l_1+1}$ and $(-1)^{l_2}$ respectively. Thus for a state of even parity in ^{17}O , l_1 is odd and l_2 is even and vice versa. Since the angular distribution for even l_1 and odd l_2 is the same as that for odd l_1 and even l_2 the parity of an isolated resonance cannot be determined from the angular distribution. Where the interference of pairs of states of the compound nucleus is involved the angular distribution depends upon the relative parity of the interfering states. In view of this the emulsions have been exposed at $E_\alpha = 4.130$ and 4.445 MeV corresponding to two resonances in addition to an intermediate energy $E_\alpha = 4.290$ MeV where the interference from the two resonances is expected to be maximum. The plates are being scanned and the preliminary data so far extracted is presented in Fig. 23.

19. Gamma ray from the Reaction $^{55}\text{Mn}(p, n\gamma)^{55}\text{Fe}$: K.V.K. Iyengar*, B. Lal* and S.K. Gupta* - The 510 and 680 KeV levels in ^{55}Fe reported by Kim¹⁾ do not seem to be generated in the $^{55}\text{Mn}(p, n\gamma)^{55}\text{Fe}$ reaction to intensities higher than 8% and 4% of the 413 KeV level. The measurements were done by observing the direct gamma-radiations with a lithium drifted germanium detector with incident photons of energy 1.80 - 3.50 MeV. The measured angular distributions of the 933 and 1322 KeV gamma-rays at $E_p = 2.40$ and 3.50 MeV and that of 1413 KeV gamma-rays at $E_p = 3.50$ MeV are in reasonable agreement with those calculated from the statistical model. The reaction proceeds through the compound nucleus, and the random phase approximation appears to be valid for the compound nucleus

* Tata Institute of Fundamental Research, Bombay.

⁵⁶Fe at these excitation energies.

1) H.J. Kim, Phys. Lett. 5 (1963) 138.

Published in Nucl. Phys. A103 (1967) 592.

20. Monte Carlo Calculations of the Energy Loss Spectra for Gamma Rays in Ge(Li) Detector: B. Lal* and K.V.K. Iyengar* - The increased use of Ge(Li) detector for gamma-ray spectroscopy has motivated theoretical calculations that predict the energy loss spectra of gamma-rays in the material for use in the design of counter system. A Monte Carlo calculation is being carried to determine the pulse height response of Ge detector to gamma rays.

The gamma-rays source is assumed to be situated on the line passing through the axis of the cylindrical detector. Photoelectric, Rayleigh scattering, Compton scattering and pair production processes have been considered for the interaction of gamma-ray in the material.

The direction of incidence of the gamma-ray on the detector face is determined by choosing at random, a vector from those uniformly distributed in the solid angle subtended by the detector on the source. The point of interaction of gamma-ray in the detector is then determined by random sampling of the exponential distribution using the total attenuation coefficient.

$$X = - \frac{1}{\mu} \ln (1 - R)$$

where X is the distance measured along gamma ray direction from the face of the detector to the point where it interacts. R is a random number

* Tata Institute of Fundamental Research, Bombay.

(between 0 and 1) and μ is the total absorption coefficient in units of cm^{-1} . Now if X exceeds the path available to the gamma-ray in the detector then the photon escapes without interaction and a count is added in a counter SE and the history is terminated. If the photon does not escape a count is added in the counter SA and the position of the point of interaction is determined. The nature of the interaction is determined by sampling the relative distributions of the various processes. The direction of scattered radiations and the associated energies are determined by sampling the appropriate distribution. The history of all the products of collision are traced in the detector until the total energy of the incident gamma-ray is accounted either by complete absorption or partly by escape of radiations. A count is placed in the appropriate channel of the energy loss histogram depending upon the fraction of the energy of the incident gamma-ray absorbed in the detector.

Since the photoelectric cross section increases rapidly as the photon energy decrease, photons below 10 KeV were assumed to be totally absorbed. For Compton events which are main source of energy degradation for the photons, the angle and energy of the scattered photons were selected from the differential Klein Nishina formula for unpolarised radiation. In photoelectric process the energy of the electron is assumed to be equal to the photon energy minus the K shell X-ray energy and the direction of the photoelectron is determined by sampling the differential distribution¹⁾

$$\frac{dx}{d\Omega} = A \sin^2 \theta \left\{ 1 + 2\beta \left(1 + \frac{E_K}{E_0} \right) \cos \theta \right\}$$

where E_k is the K, X-ray energy and $E_e = h\nu - E_k$ the azimuthal angle of the electron and the direction of the X-ray is determined by random sampling.

In Rayleigh scattering about 75% of the scattering is known to be within a small forward angle θ_c , within which the distribution varies very rapidly $\theta_c = 2\text{Sin}^{-1} (0.026 Z^{1/3} m_0 c^2 / h\nu)$ and beyond θ_c it varies slowly and goes down as the angle increases²⁾. Since no definite form of the distribution is known it has been assumed in the calculations that if the event is scattered within θ_c then the polar angle is $\sim \frac{\theta_c}{2}$ and if it is beyond θ_c then the angle is determined by random sampling from the region $180^\circ - \theta_c$. This approximation does not introduce much error since the over all cross section of the process is anyway quite small compared with photoelectric process at low energies where the Rayleigh scattering is significant.

In pair production the excess of kinetic energy is equally distributed between the electron and positron and the directions of the electron or positron with respect to the incident photon is taken to be³⁾

$$\theta_{\pm} = \frac{m_0 c^2}{E_{\pm}}$$

where $E_{\pm} = 1/2 (h\nu - 2m_0 c^2)$ and the azimuthal angles for one of them is determined by random sampling and for the other particle it differs by 180° . Figure 24 shows the schematic flow diagram of the calculations.

The calculations outlined above do not take into account the resolution effects within the crystal and its amplification. Auxiliary calculations has been made to obtain the broadening of the full energy peak

by application of Gaussian resolution function with an empirically determined half width for comparison of the response function with the experimental obtained spectrum.

A programme is being written for CDC - 3600 computer to compute the intrinsic efficiency of the detector, the photo to total ratio of the spectrum and the energy loss spectrum for cylindrical germanium detectors.

- 1) A.H. Compton and S.K. Allison, X-Rays in Theory and Experiment, D. Van Nostrand Co., Princeton, N.J. (1935), Second Edition, p. 579.
- 2) P.B. Moon, Proc. Phys. Soc. (London) A63 (1950) 1189.
- 3) H.A. Bethe and J. Ashkin, Passage of Radiation through Matter, Experimental Nuclear Physics, John Wiley and Sons, Inc., New York (1953) Vol. I.

21. Gamma-rays from $^{75}\text{As}(p, n\gamma)^{75}\text{Se}$: K.V.K. Iyengar*, P.J. Bhalerao, M.Y. Vaze and B. Lal* - Spectra of gamma-rays from the proton bombardment of arsenic evaporated on gold foil have been taken using NaI(Tl) and Ge(Li) detectors at several proton energies in the region 3.0 to 5.0 MeV with a view to obtain information on the energy level of ^{75}Se . The yield of Gamma-rays from ^{75}As was found to be quite low compared to the background gamma-rays from gold backing. It is proposed to use self supporting targets of ^{75}As to study the gamma-rays from $^{75}\text{As}(p, n\gamma)^{75}\text{Se}$ and obtain their angular distribution. The information available on the level scheme of ^{75}Se is at present very limited, and it is hoped that these studies will lead to additional information on the level structure of ^{75}Se .

* Tata Institute of Fundamental Research, Bombay.

INSTRUMENTATION

1. Charged Particle-Gamma Ray Angular Correlation Goniometer for Studies in Nuclear Reactions: M.A. Eswaran, P.C. Mitra and N.L. Ragoowansi -

A charged particle-gamma ray angular correlation goniometer has been set up in the beam room at the left beam port. The major parts of the assembly are the following:

1. A 11 cm. diameter target chamber with thin (0.8 mm) stainless steel wall, in which semiconductor charged particle detector can be mounted at 0° to the beam or an annular detector at 180° . The angular orientation and the vertical position of the target are adjustable without breaking the vacuum. Lead shielded tantalum beam collimators are also incorporated. The chamber is supported by adjustable screw assembly from the top in a cantilever arrangement.
2. Gamma-ray detector assembly comprising of 12.7 cm x 15.2 cm long NaI(Tl) scintillation detector mounted on XP 1040 phototube with 2.5 cm thick and 18 cm long lead shielding mounted on a arm which can rotate about the vertical axis, fixed on a table supported on levelling screws. The axis of rotation of the gamma detector can be aligned to coincide with the vertical axis passing through the beam spot on the target in the chamber. The distance and height of the gamma detector are adjustable by screw arrangement. Graduations are provided for every 0.5 degree for the position of the γ - detector.

A liquid nitrogen cold trap to reduce the amount of carbon build up on the target during beam bombardment is incorporated and a quartz viewer is also provided in the assembly to facilitate beam tube alignment.

A schematic diagram of the whole assembly along with the pumping system, is shown in figure 25.

2. Optimum Parameters for a Constant Deviation Magnetic Spectrograph:

M.N. Viswesvariah and N. Sarma - The constant deviation magnetic spectrograph proposed originally by Borggreen¹⁾ et al, was generalised so as to give optimum parameters for 28 different spectrographs with a variable range ion optical properties like energy resolution, dispersion, magnification and transmission.

A variational calculation of the r.m.s. aberration over the focal plane was done by changing one machine parameter at a time and optimisation was done by looking for the combination of machine parameters giving the smallest of the r.m.s. aberration along the focal plane.

The results of these calculations have been published in the Report B.A.R.C. - 320 (1967).

- 1) J. Borggreen, B. Elbeck and L. Perch Nielsen, Nucl. Instr. and Meth. 24 (1963) 1.

To be published in Nucl. Inst. and Methods.

3. A Recoil Proton Counter for Fast Neutron Flux Measurement:

G. Muthukrishnan*, K.B.S. Murthy* and C.M. Sunta* - A counter for fast neutron flux measurement has been developed with uniform response from 0.5 to 14.0 MeV using the technique of recoil-proton counting. The counter is filled with a hydrogenous gas (Burshane) and lined inside with polythene sheets of two different thicknesses (0.02 mm and 0.8 mm) which

* Health Physics Division, B.A.R.C.

act as proton radiators. The energy response of the counter has been tested experimentally using monoenergetic neutrons produced by bombarding tritium targets with proton beam from the 5.5 MeV Van de Graaff accelerator.

Published in Nucl. Instr. and Methods 55 (1967) 269.

4. A Current Integrator for Use with Low Variable Currents: S.K. Gupta*-

A transistorized current integrator using a very high input impedance has been designed. It is found to be linear in the range 1 nA to 10 μ A. The leakage has been reduced to $\sim 5 \times 10^{-12}$ amps. and reproducibility of the calibration is within $\pm 0.3\%$.

Published in Nucl. Inst. and Methods 60 No. 3 (1968) 323.

5. A Mass Identifier System For Charged Particles: S.K. Gupta*,

M.G. Betigeri and S.N. Misra - A telescope consisting of a 100 μ m transmission type ΔE silicon detector and an 800 μ m E silicon detector has been assembled. For a charged particle passing through the ΔE detector and losing all its remaining energy in the E detector a product pulse $P = K \Delta E (E + F \Delta E + E_0)$ is electronically stimulated. If the values of F and E_0 are suitably adjusted the product P is proportional to mZ^2 of the particle. As the solid state detectors have got linear energy response independent of the particle type, it is simple to calculate the values of F and E_0 using a Fortran program. The program linearly least square fits the above expression. Minimizing,

$$X^2 = \left[mZ^2 - \left\{ A \Delta E \cdot E + B (\Delta E)^2 + C \Delta E \cdot E_0 \right\} \right]^2$$

* Tata Institute of Fundamental Research, Bombay.

The ratios $\frac{B}{A}$ and $\frac{C}{A}$ give the values of the constants F and E_0 for the energy range and the type of particles chosen. Having obtained these constants they are adjusted using energy calibrated pulsers.

The electronics block diagram is given in Fig. 26. We use Ortec 103-203 systems to generate flat top pulses using them in delay line mode. Discriminators in E and ΔE channels are set according to the energy range and particles desired. Electronically F is variable between 0 and 1 and E_0 can be set either positive or negative. Log conversion is achieved by using transistors 2N414. The circuit within dashed lines is the multiplier circuit generating log P. This circuit has been fabricated. Using other available electronic circuitry the performance of the system has been checked and it has been found to be working satisfactorily. The system has already been used in the preliminary run of (n,d) and (n,p) reactions at $E_n = 14$ MeV. It has been further planned to use it in (d,p) and ($^3\text{He},p$) reactions.

INDIAN NUCLEAR DATA GROUP

M. Balakrishnan (Secretary), H.G. Devare*, A.S. Divatia (Convener), S.S. Kapoor, D.N. Kundu**, C.S. Pasupathy, B.P. Rastogi and N.S. Satya Murthy.

1. Participation in IAEA Activities:

a. Progress Report on Nuclear Data Activity - A report entitled "Progress Report on Nuclear Data Activities in India IV" (BARC - 305) was compiled and published in October 1967.

b. CINDA (Computer Index Neutron Data) - Journals and reports from India were covered for information relevant to nuclear data and 54 entries were sent to the Nuclear Data Unit.

c. DASTAR (Data Storage and Retrieval System) - Data on (n,p) , (n,α) and (n,γ) reactions were contributed to the DASTAR. Total number of entries from Indian Laboratories is 10.

d. Reports submitted to International Nuclear Data Committee - Seven BARC reports have been submitted to IAEA as INDG documents.

2. Measurement Programme: At the Van de Graaff Laboratory, following experiment of interest in the Nuclear Data field have been undertaken by various groups:

a. (α,n) and (p,n) reactions

i) $^{29}\text{Si}(\alpha,n)^{32}\text{S}$

ii) $^{51}\text{V}(p,n)^{51}\text{Cr}$

* Tata Institute of Fundamental Research, Bombay.

** Saha Institute of Nuclear Physics, Calcutta.

b. Fast neutron induced fission of ^{235}U .

The values of angular anistoropy of fragments in binary and ternary fission induced by 3 MeV neutron are found to be 1.17 ± 0.2 and 0.89 ± 0.10 respectively.

Details will be found lesewhere in this report.

SEMINARS

A series of lectures on resonance theory of nuclear reaction and the mechanism of direct reactions were given by M.K. Mehta and N. Sarma respectively. A.S. Divatia covered the "Theory of Cyclic Accelerators" in another series of lectures. N. Nazakat Ullah, (TIFR) gave three lectures on "Compound Nuclear Resonance Structure". Coincidence techniques in nuclear reaction experiments were covered in two lectures by N.L. Ragoowansi and P.J. Bhalerao. Other subjects covered during the weekly seminars held at the laboratory include "Door way states in nuclear reactions".

LIBRARY

The Physics Group Library at the Vande Graaff Laboratory has registered a further growth. The necessity of a users guide was felt all the more and its preparation is now nearing completion.

Library Collection:

950 books and 403 bound volumes have been received during the period under report. The library has now 4196 books and 2224 bound volumes and periodicals (6440 volumes in all compared to 5087 at the end of 1966). This excludes B.A.R.C. reports and reprints which also registered an increase over the previous period.

Indian Nuclear Data Group:

123 full size reports were received during this period bringing the total to 267. Lists of these reports are sent to various laboratories and scientific institutions in India from time to time.

Publications by Nuclear Physics Division:

A complete list of papers and reports published by the staff of the Nuclear Physics Division, BARC from 1951 - 1967 has been compiled and will be published shortly.

Library Hours:

The working hours of the library have been extended. The library now works from 9.00 hrs to 18.30 hrs.

UTILISED FOR RESEARCH EXPERIMENTS
PERCENTAGE OF MAXIMUM POSSIBLE EXPERIMENTAL TIME

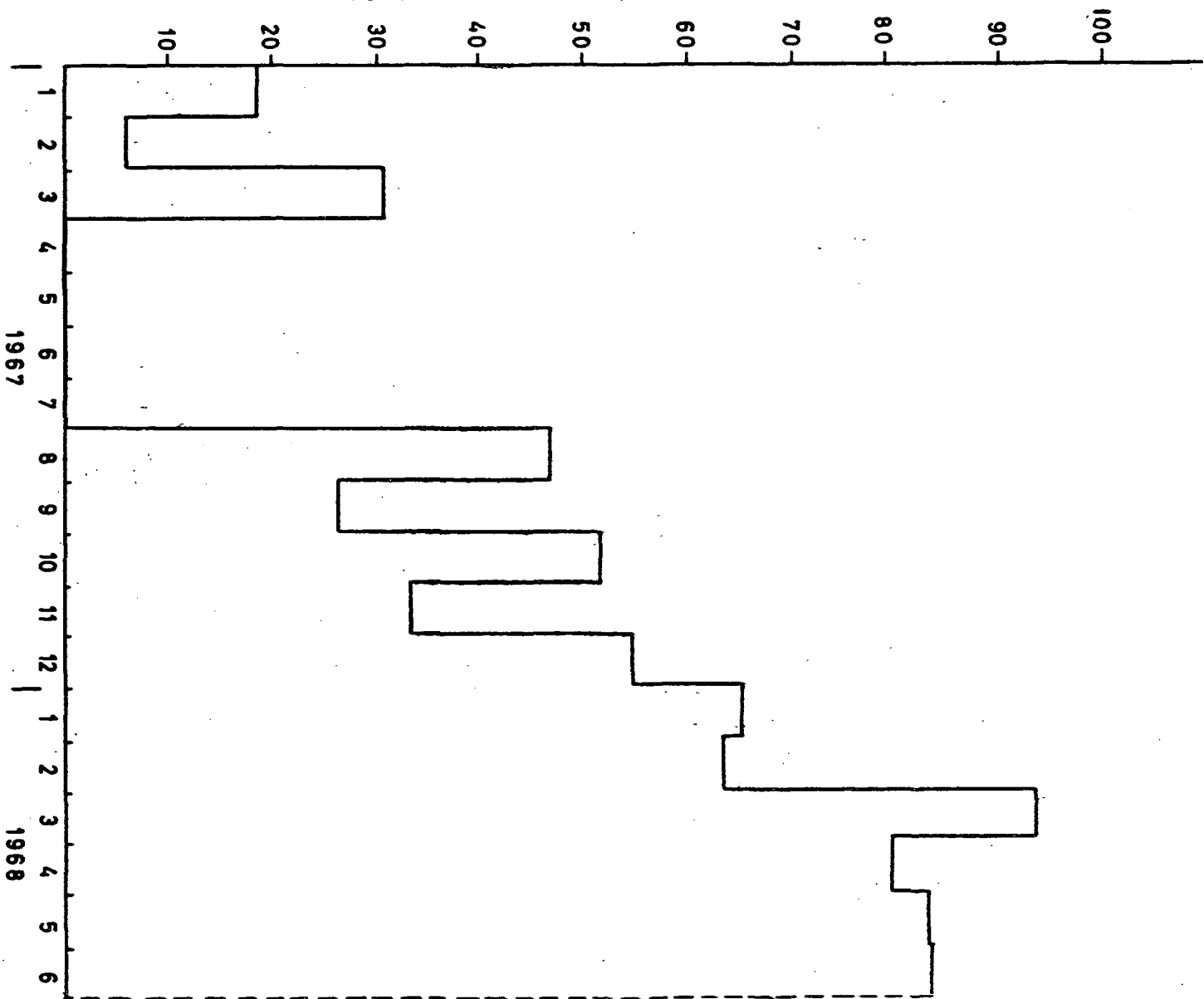


FIG. 1

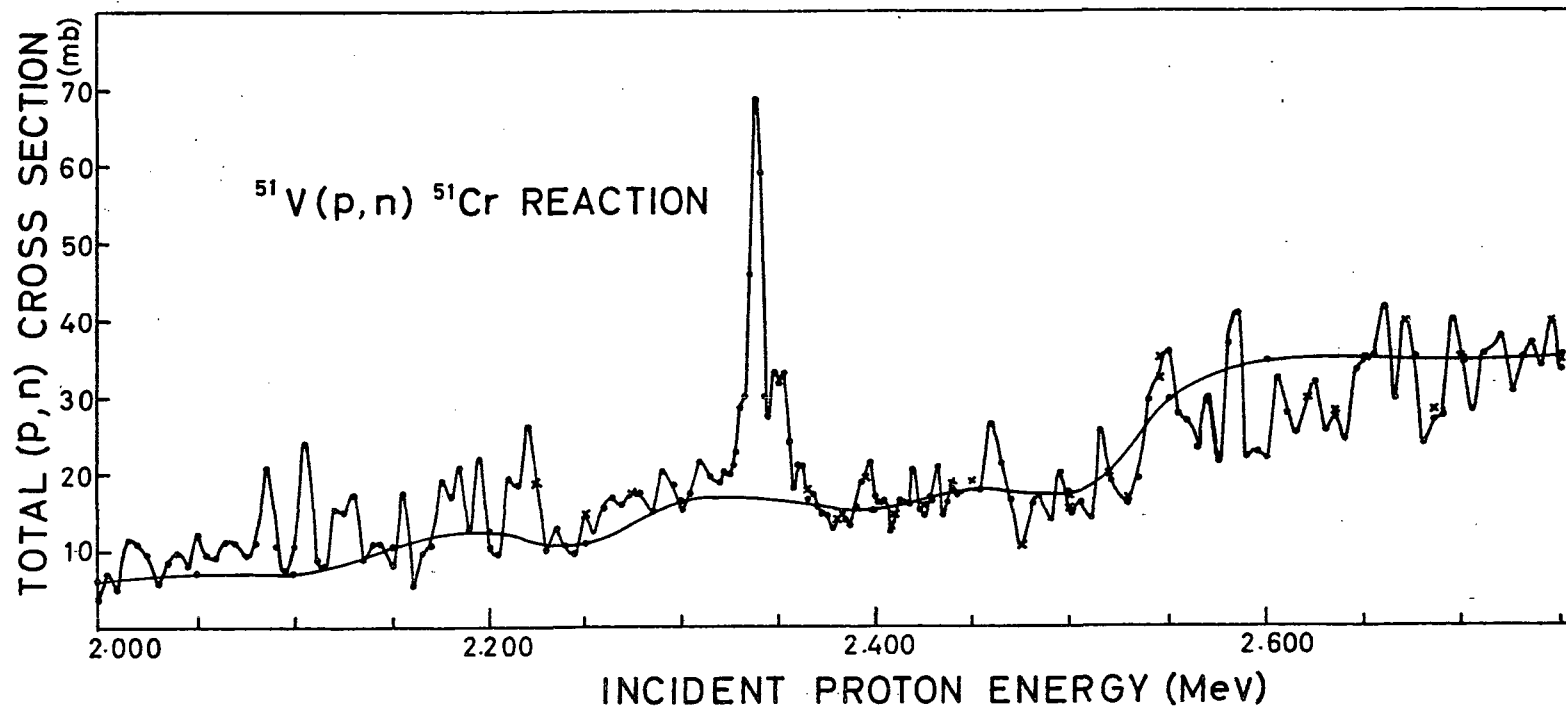


FIG-2

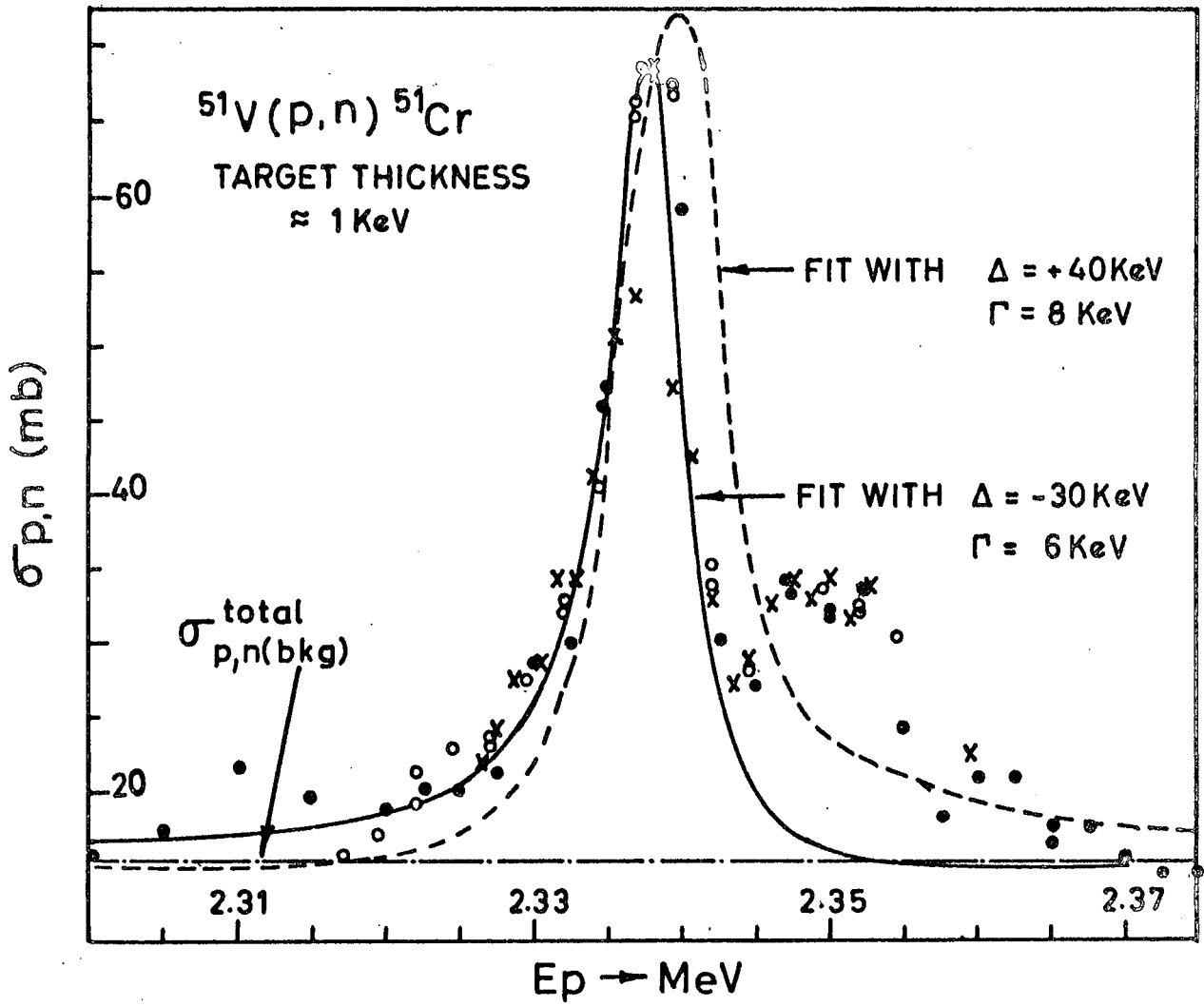


FIG-3

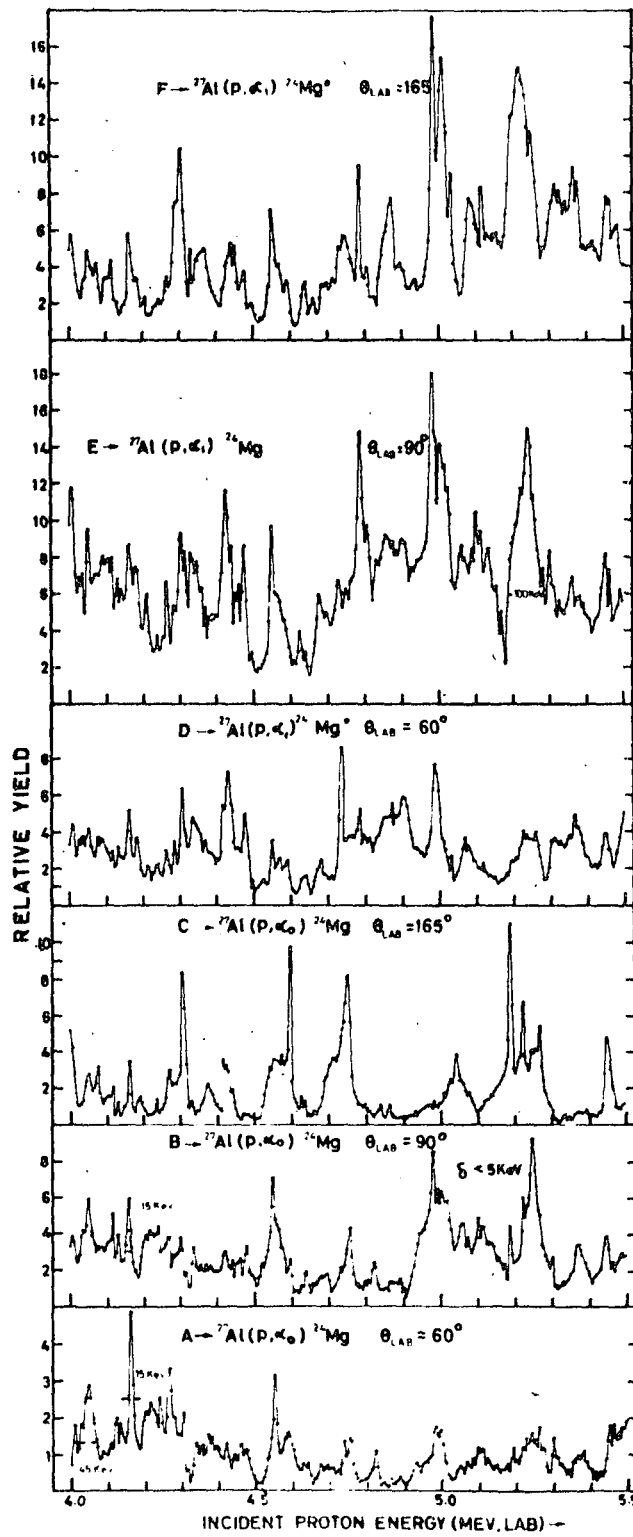


FIG-4

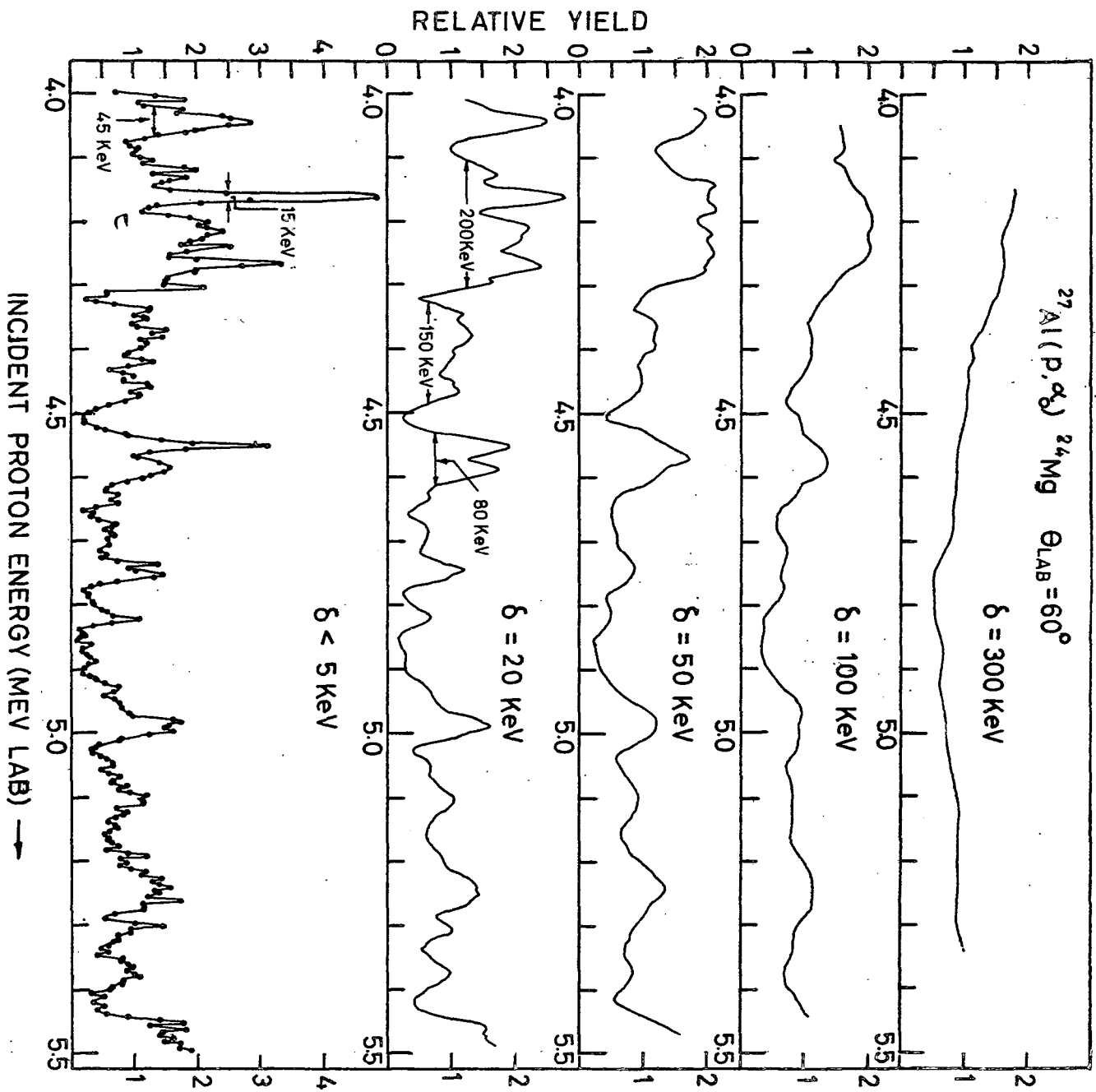


FIG-5

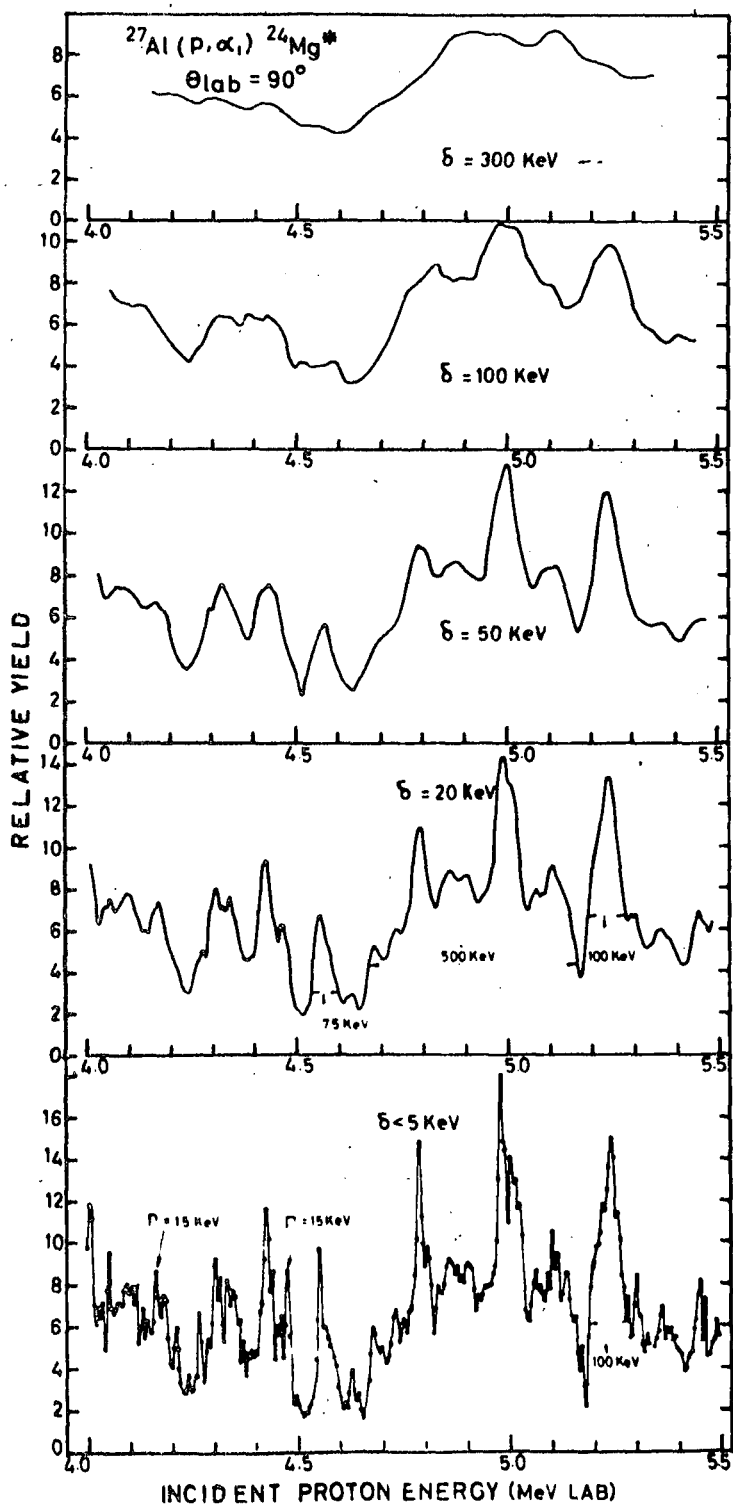
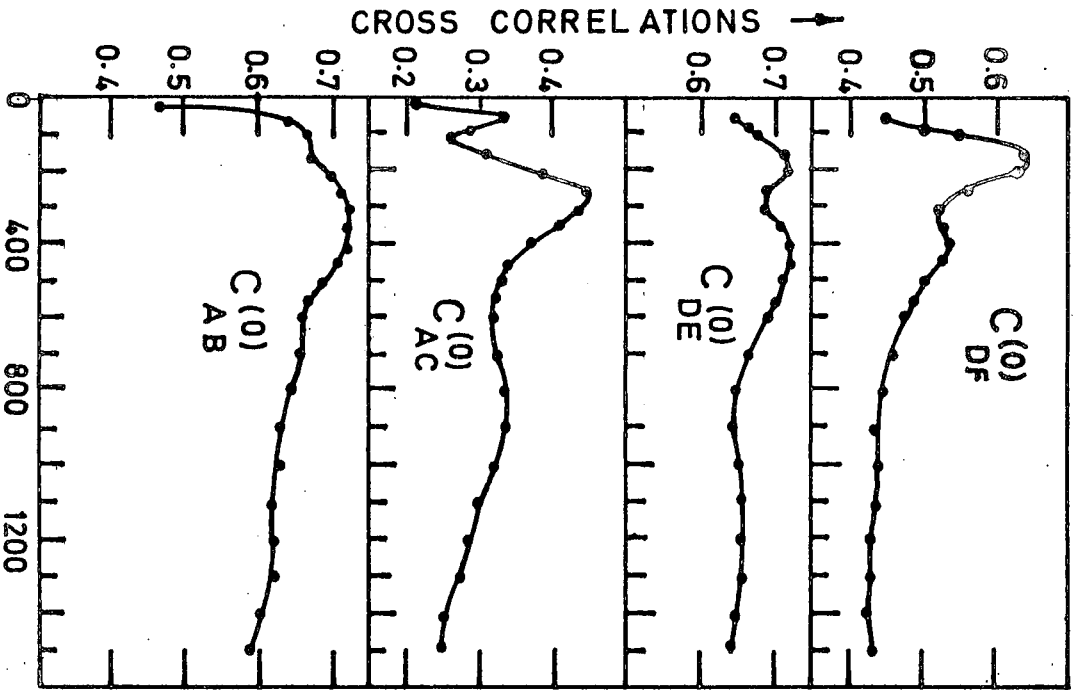


FIG - 6

ANGULAR CROSS CORRELATIONS



CHANNEL CROSS CORRELATION

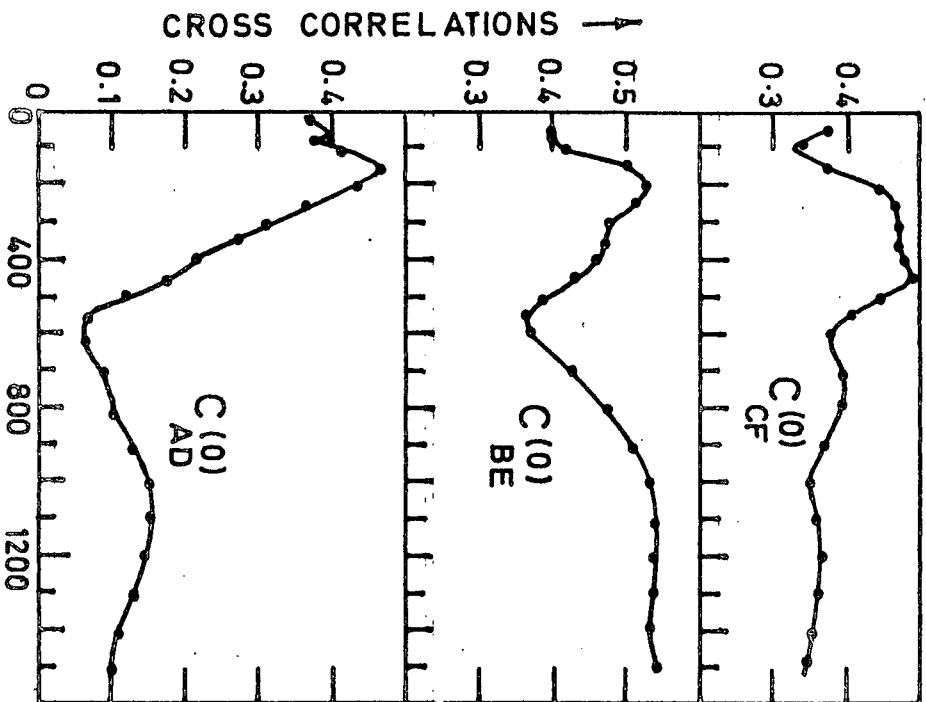


FIG-7

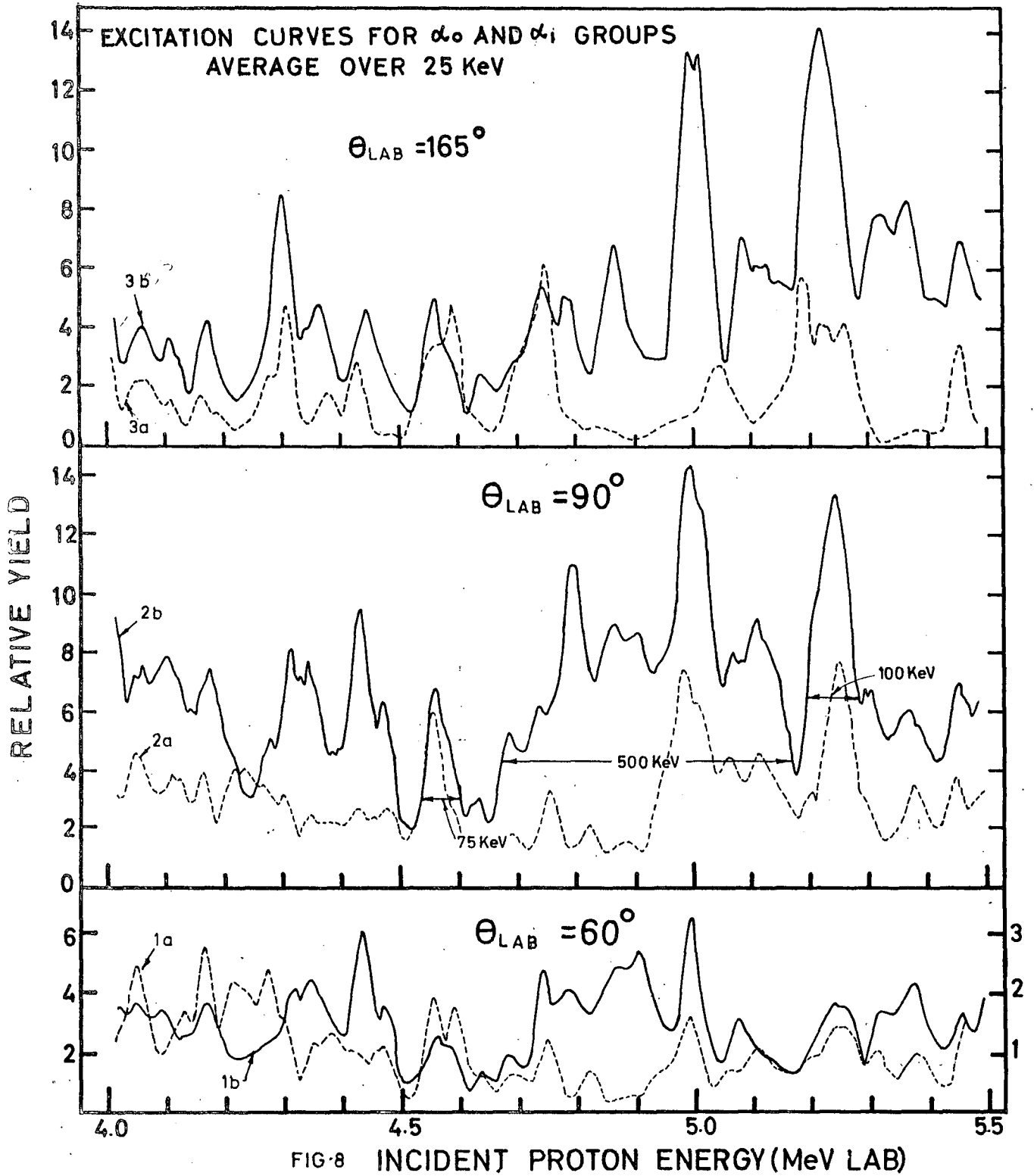
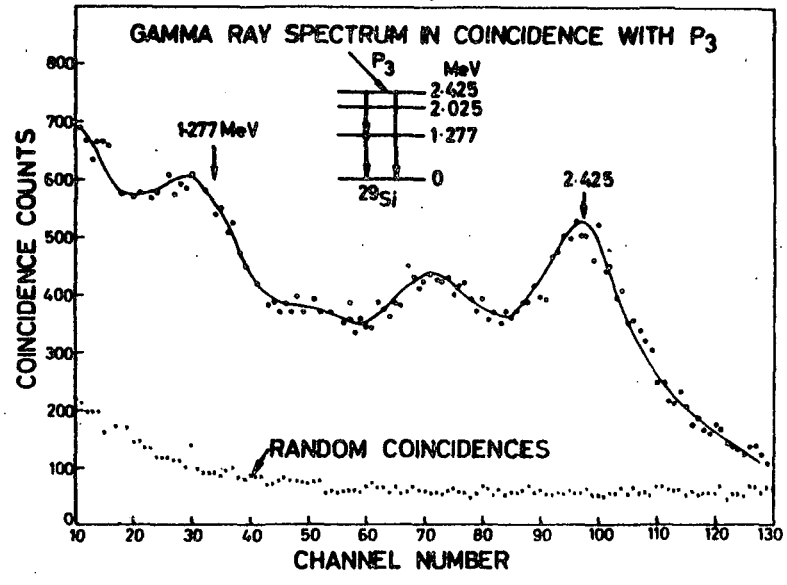


FIG-8 INCIDENT PROTON ENERGY (MeV LAB)

$^{28}\text{Si}(d,p\gamma)^{29}\text{Si}$



$^{28}\text{Si}(d,p\gamma)^{29}\text{Si}$

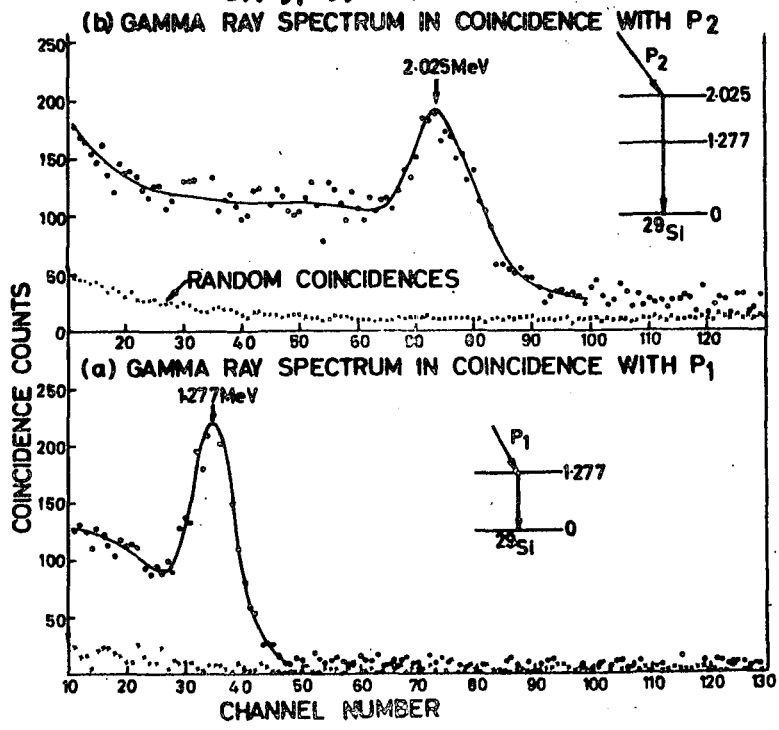


FIG - 9

$^{28}\text{Si}(d, p\gamma)^{29}\text{Si}$

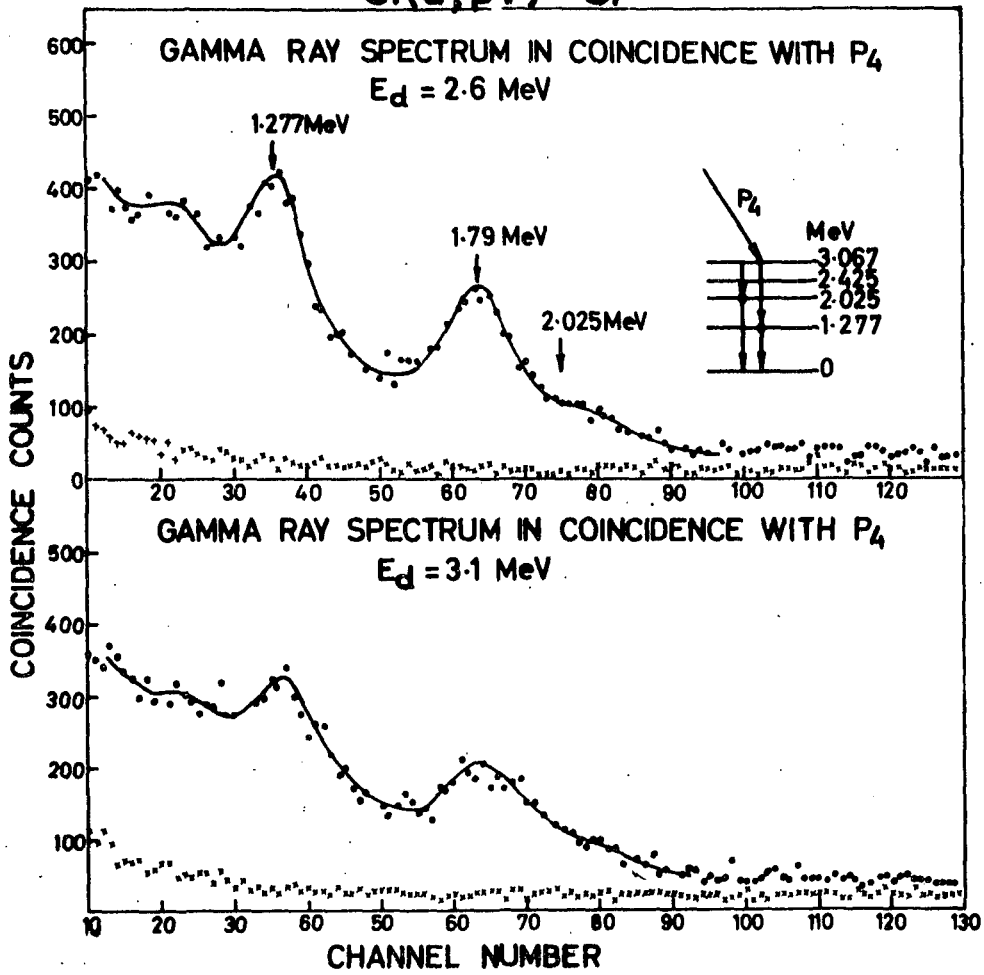


FIG -10

$^{28}\text{Si}(d, p \gamma)^{28}\text{Si}$

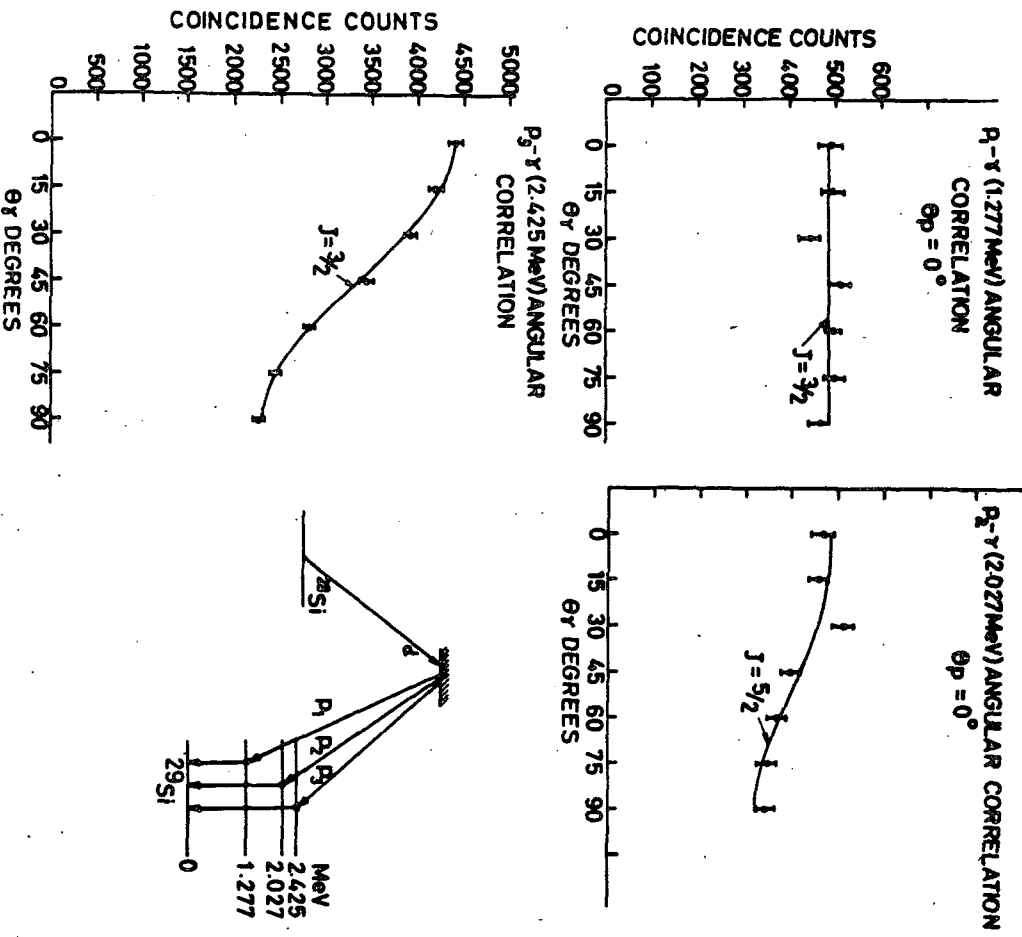


FIG-11

$^{28}\text{Si}(d, p_4 \gamma)^{29}\text{Si}$

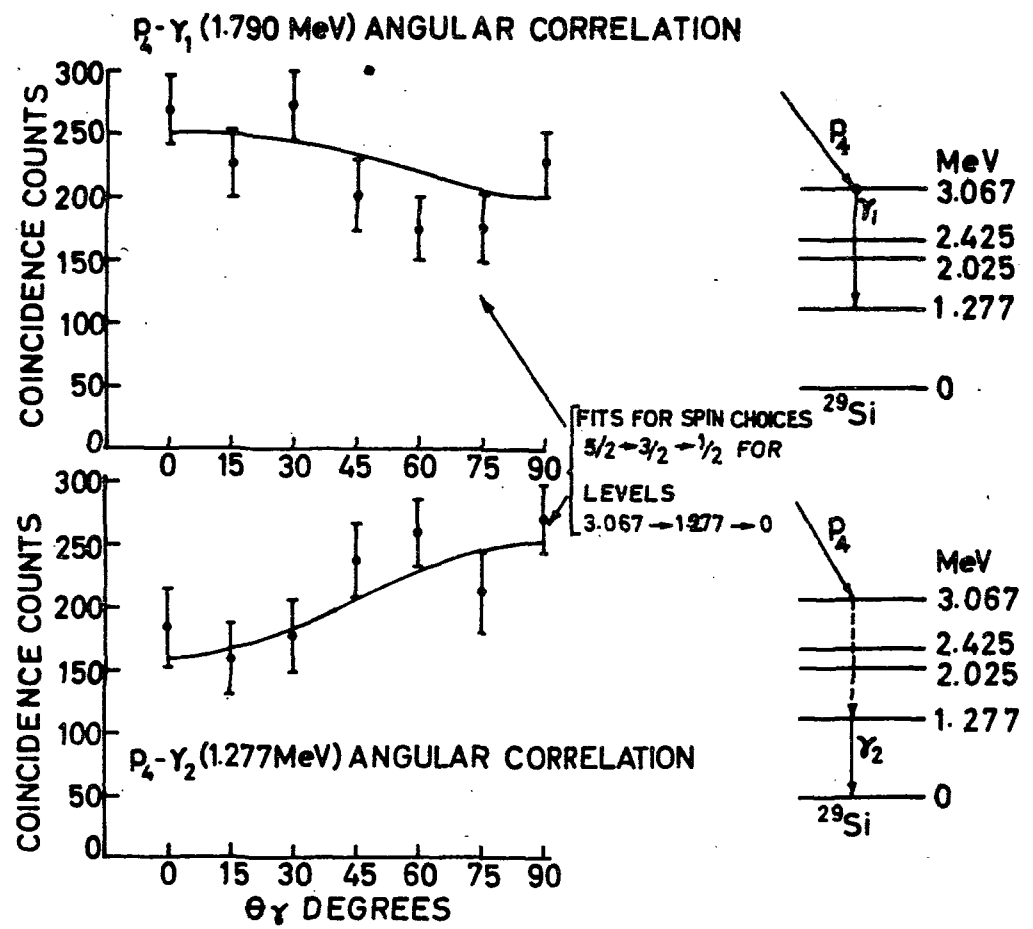


FIG-12

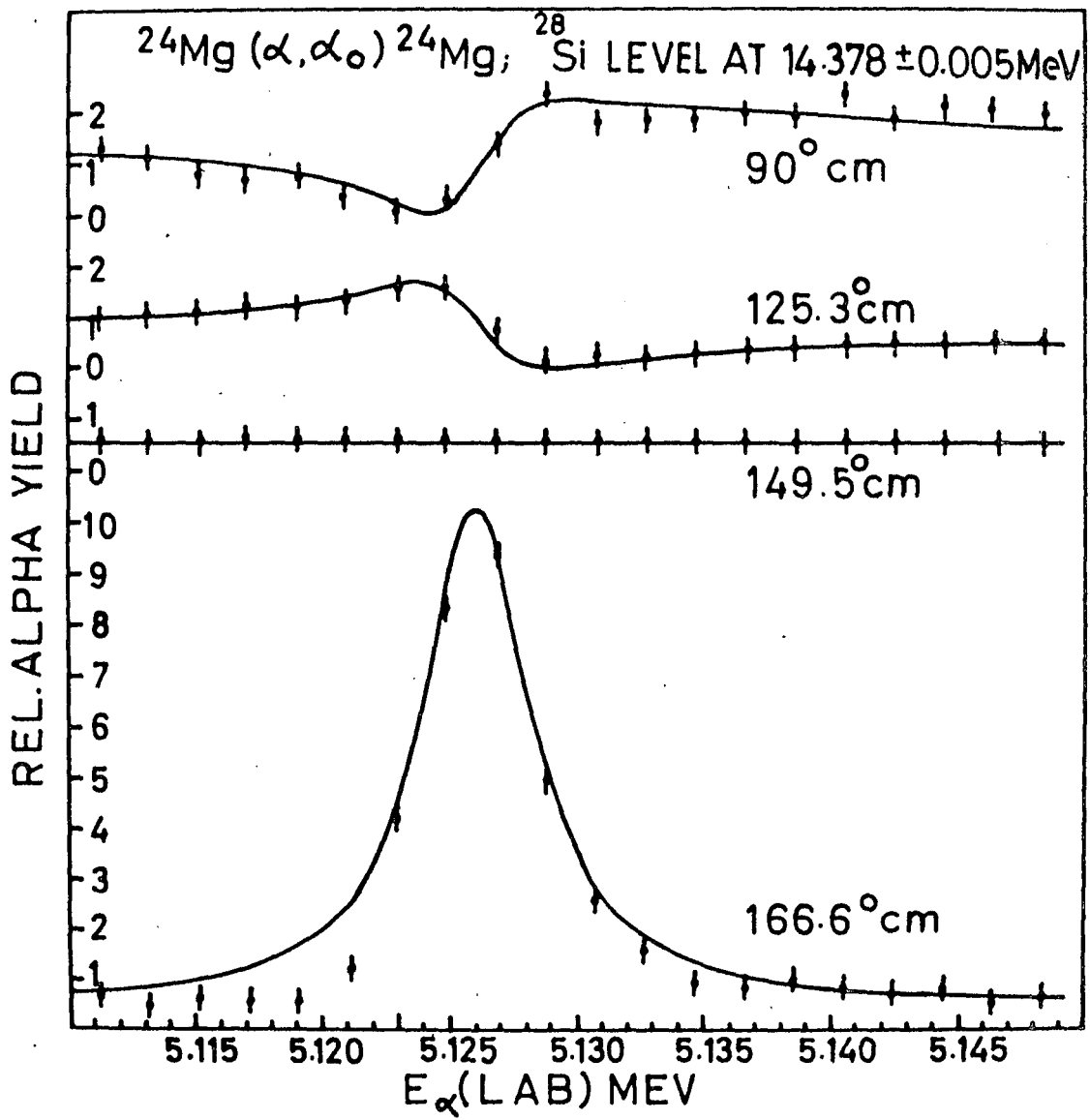


FIG-13

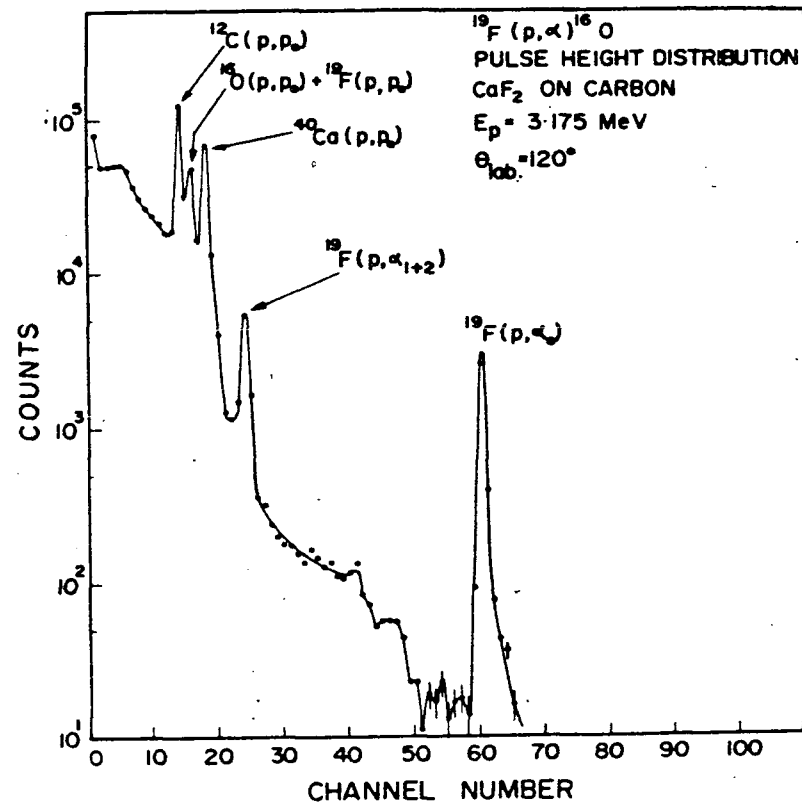


FIG-14

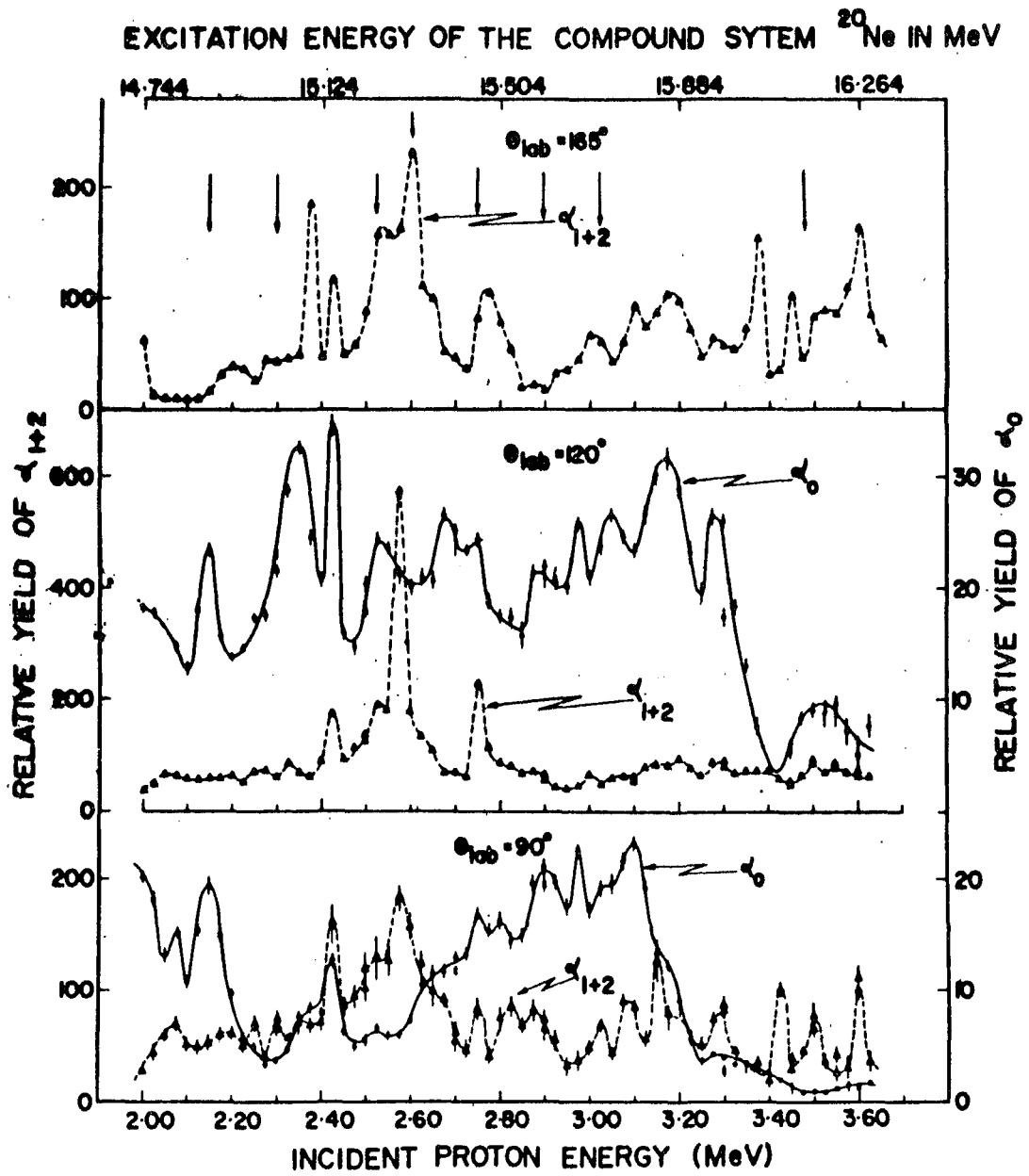


FIG-15

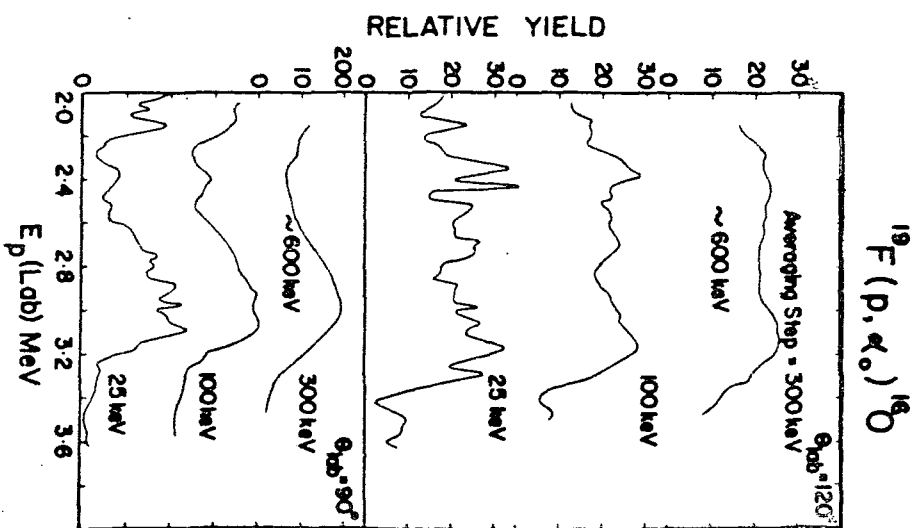
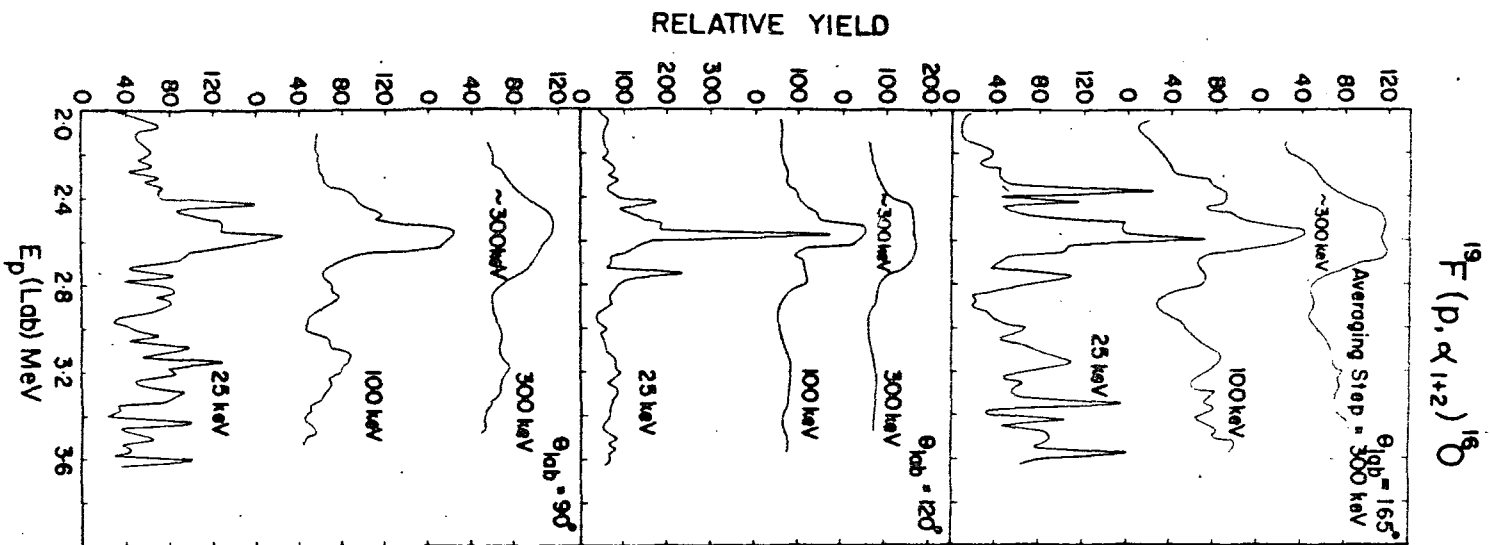


FIG-16

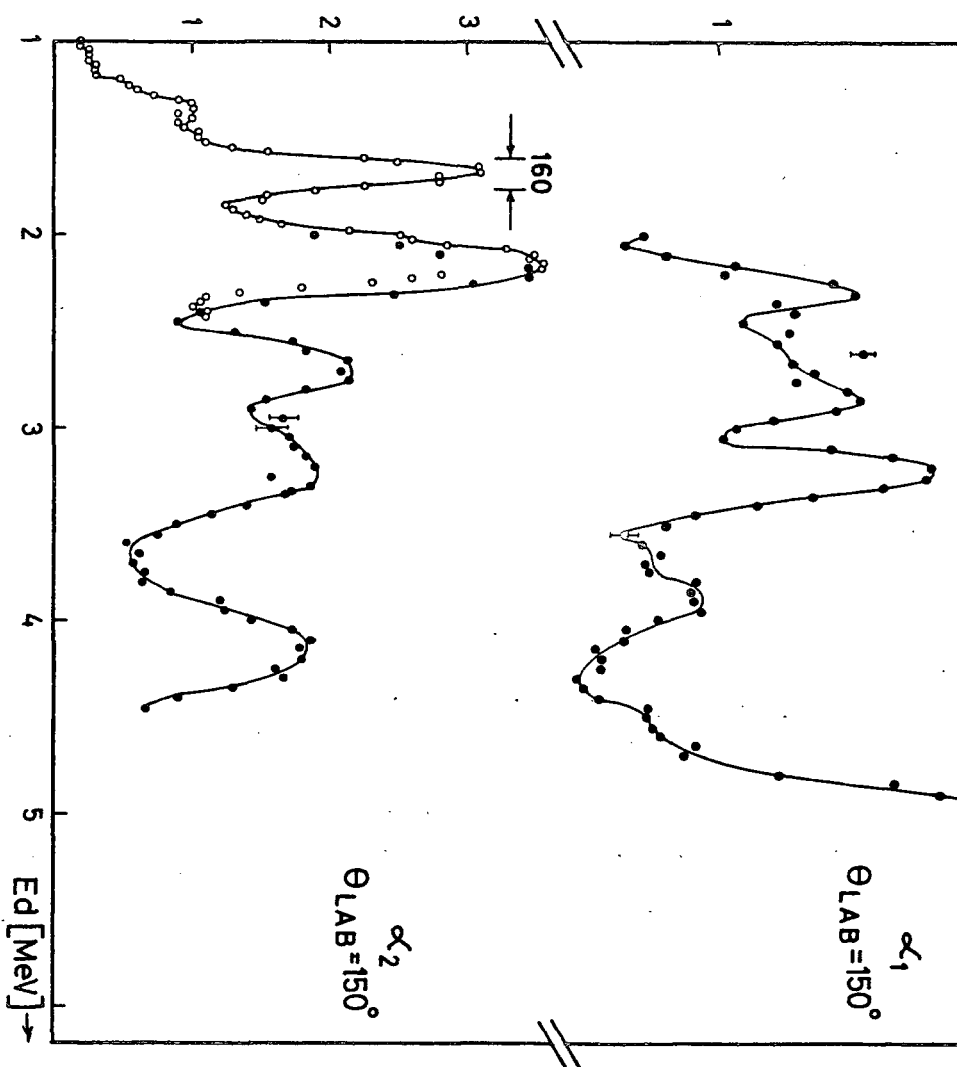
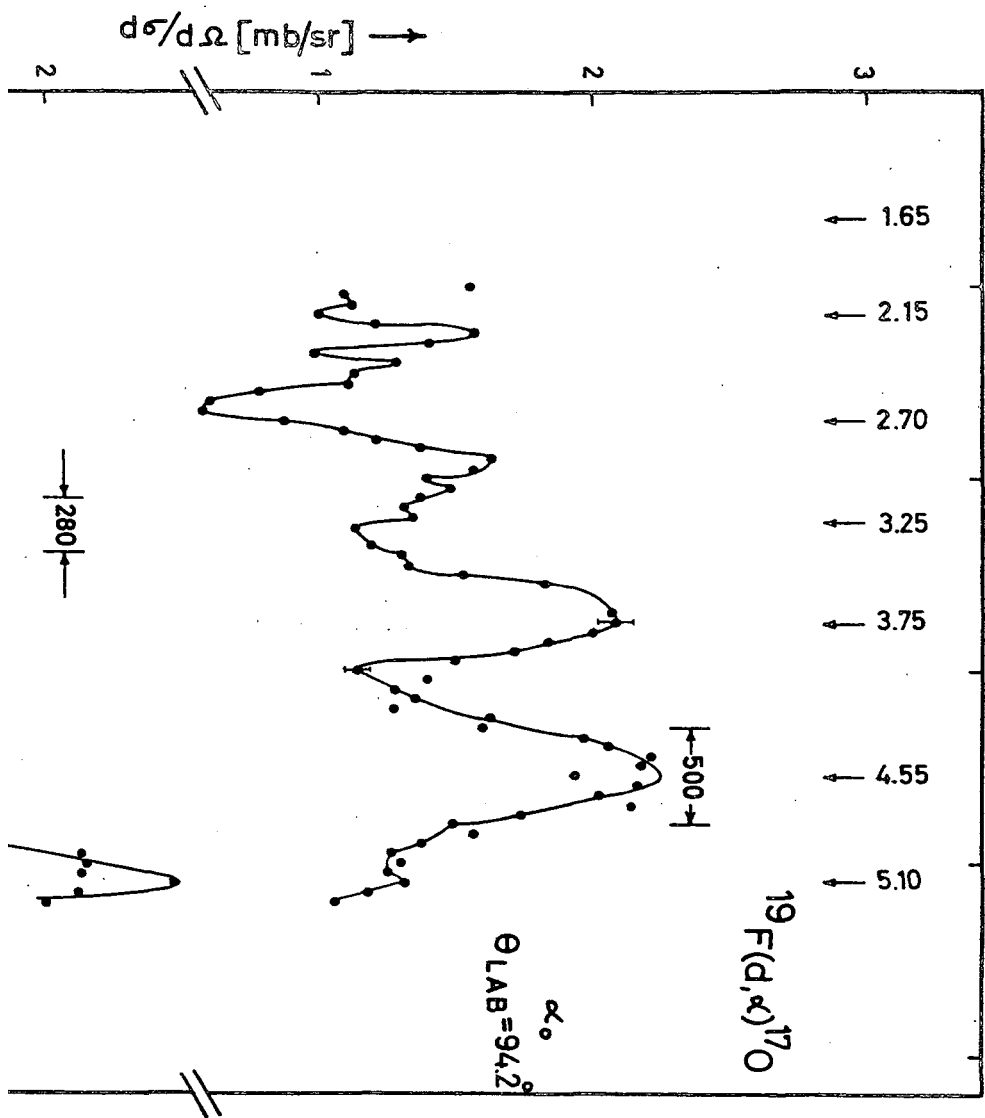


FIG-17



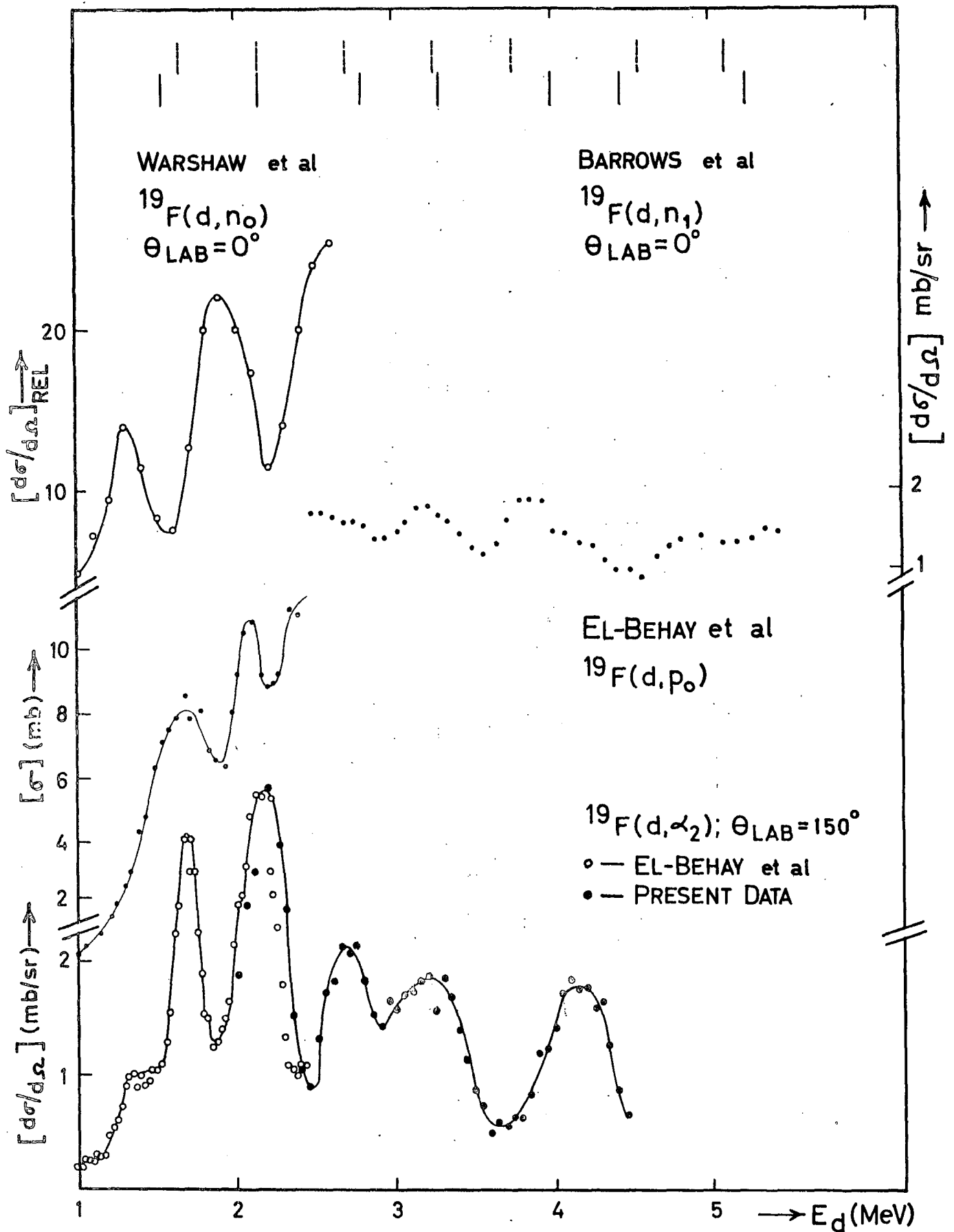


FIG 18

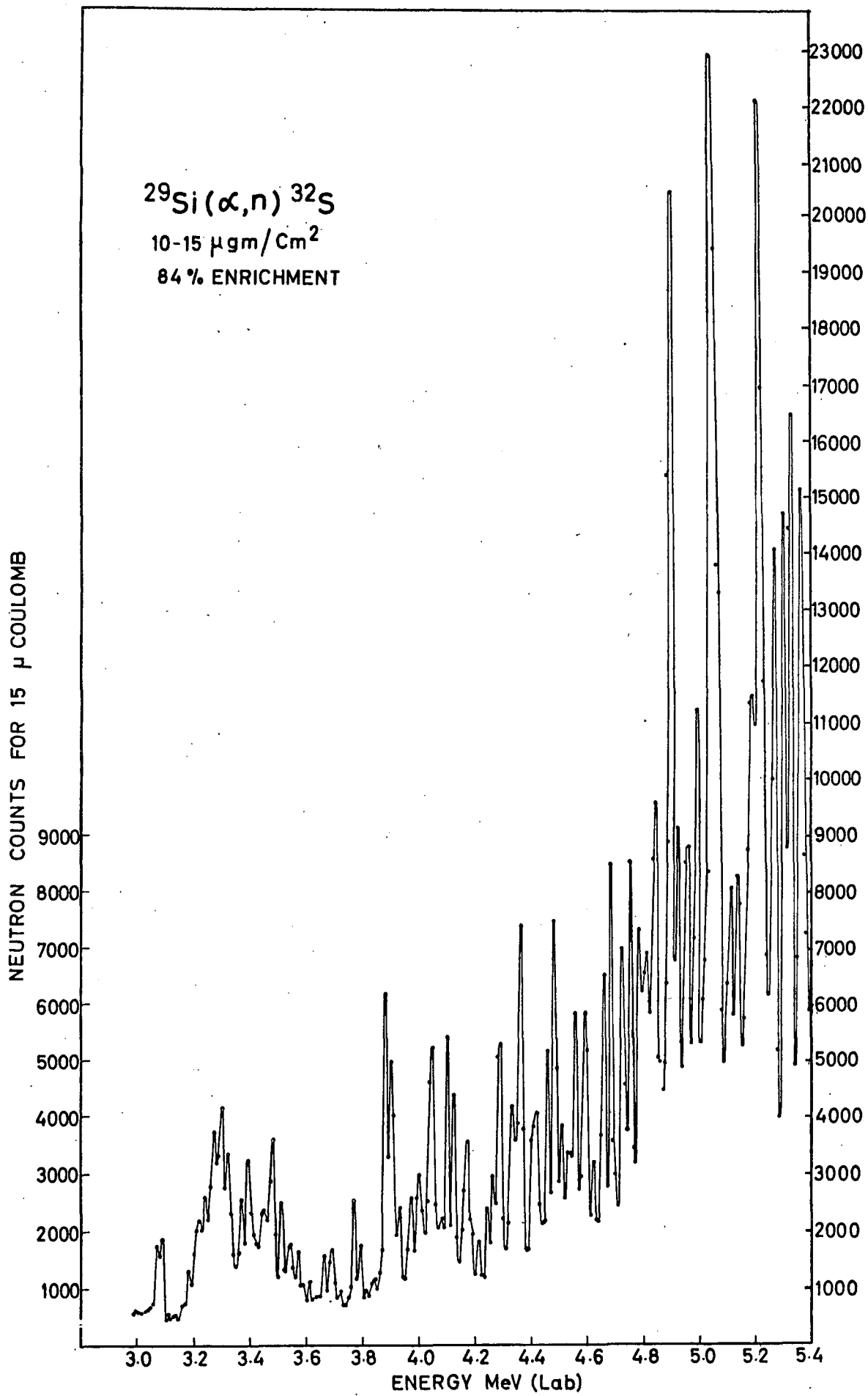


FIG-19

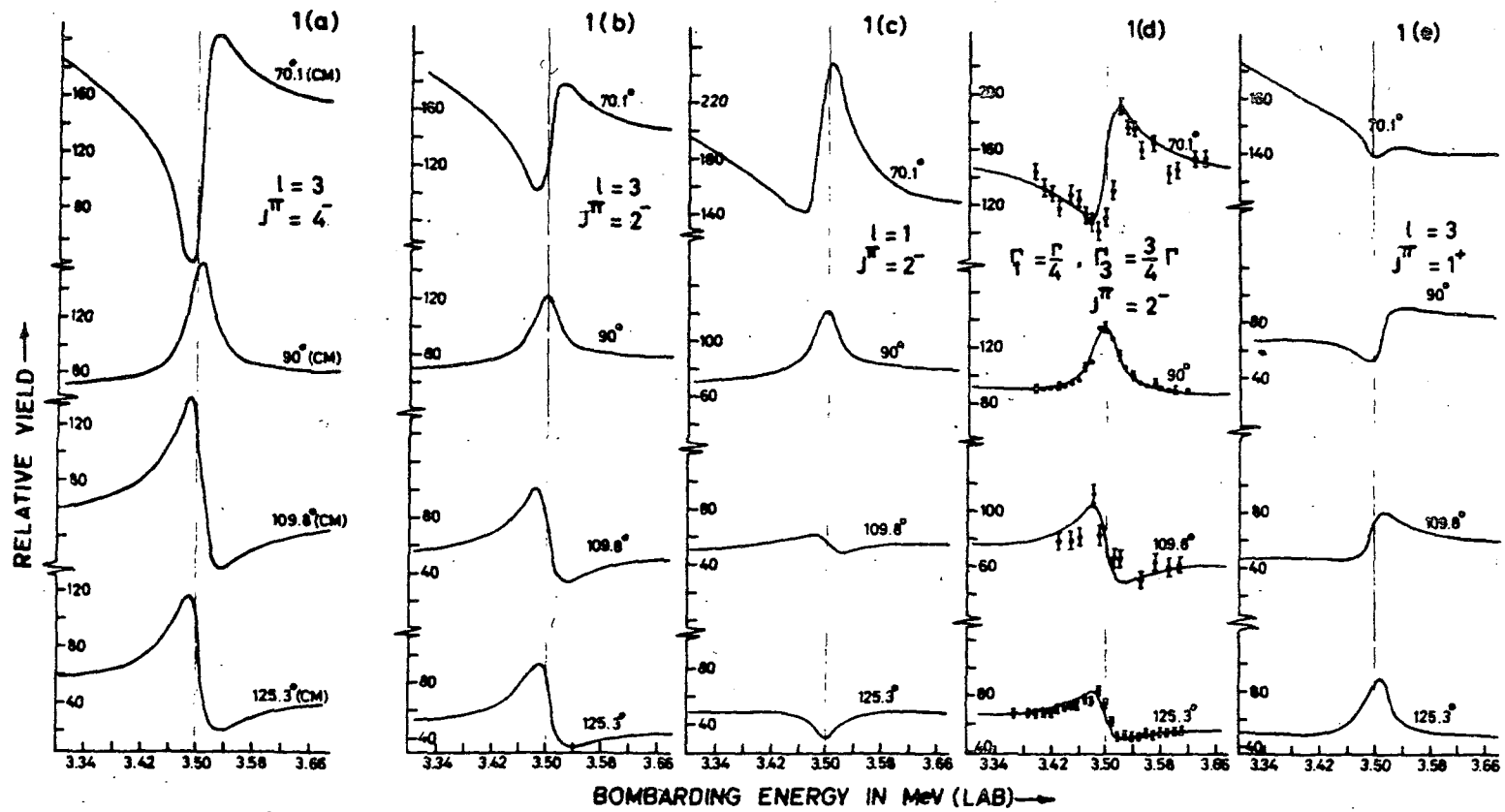


FIG. 1 THEORETICAL AND EXPERIMENTAL EXCITATION FUNCTION FOR $E_m=3.50$ MeV

FIG-20

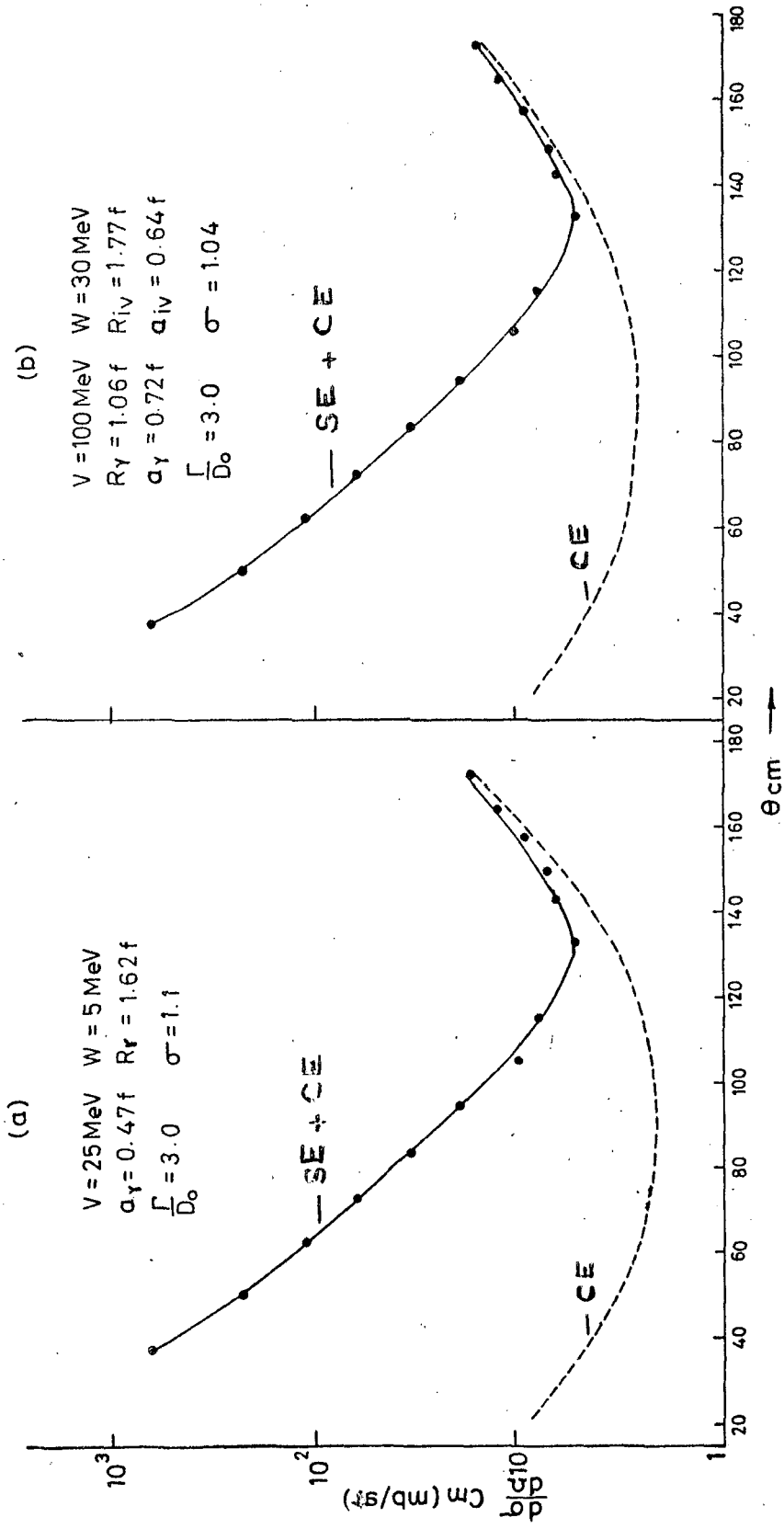


FIG. 21

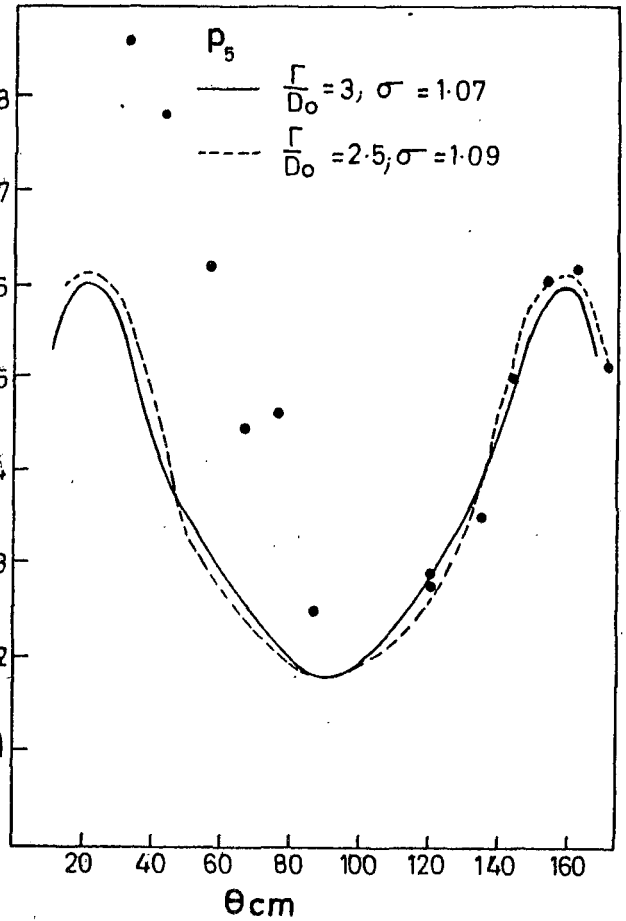
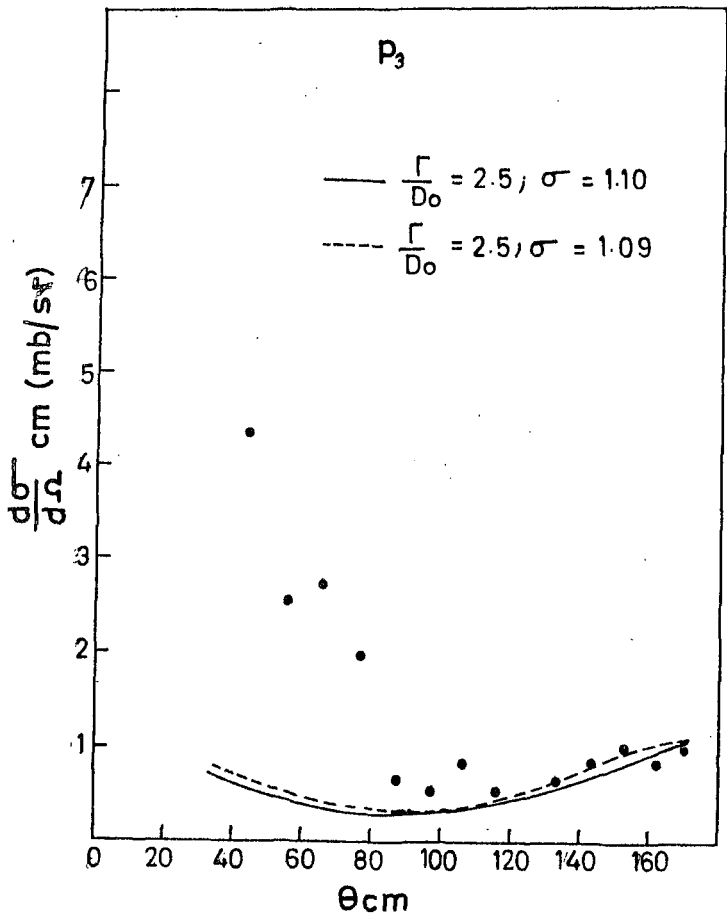
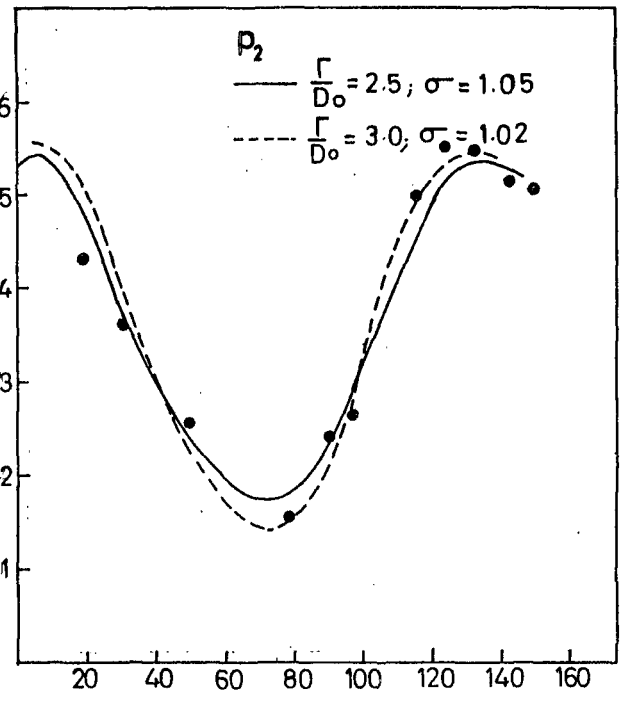
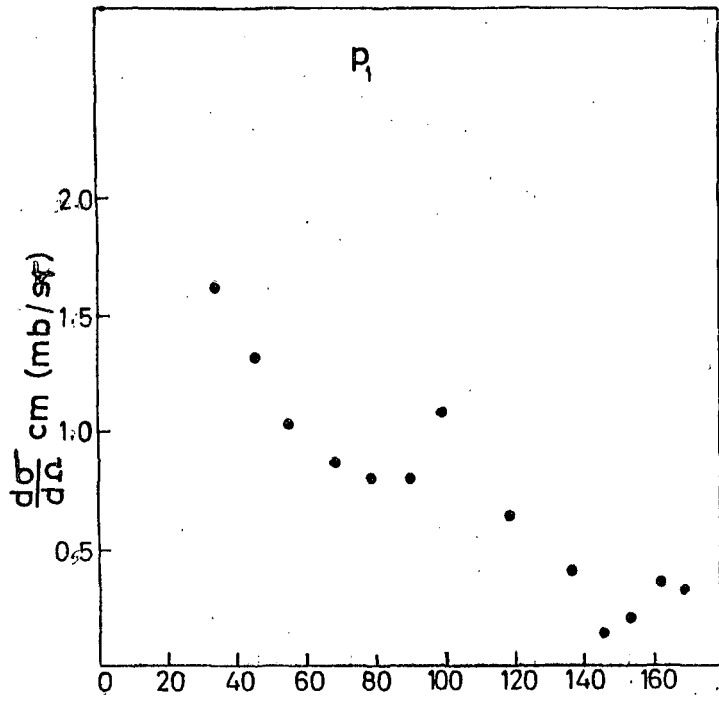


FIG. 22

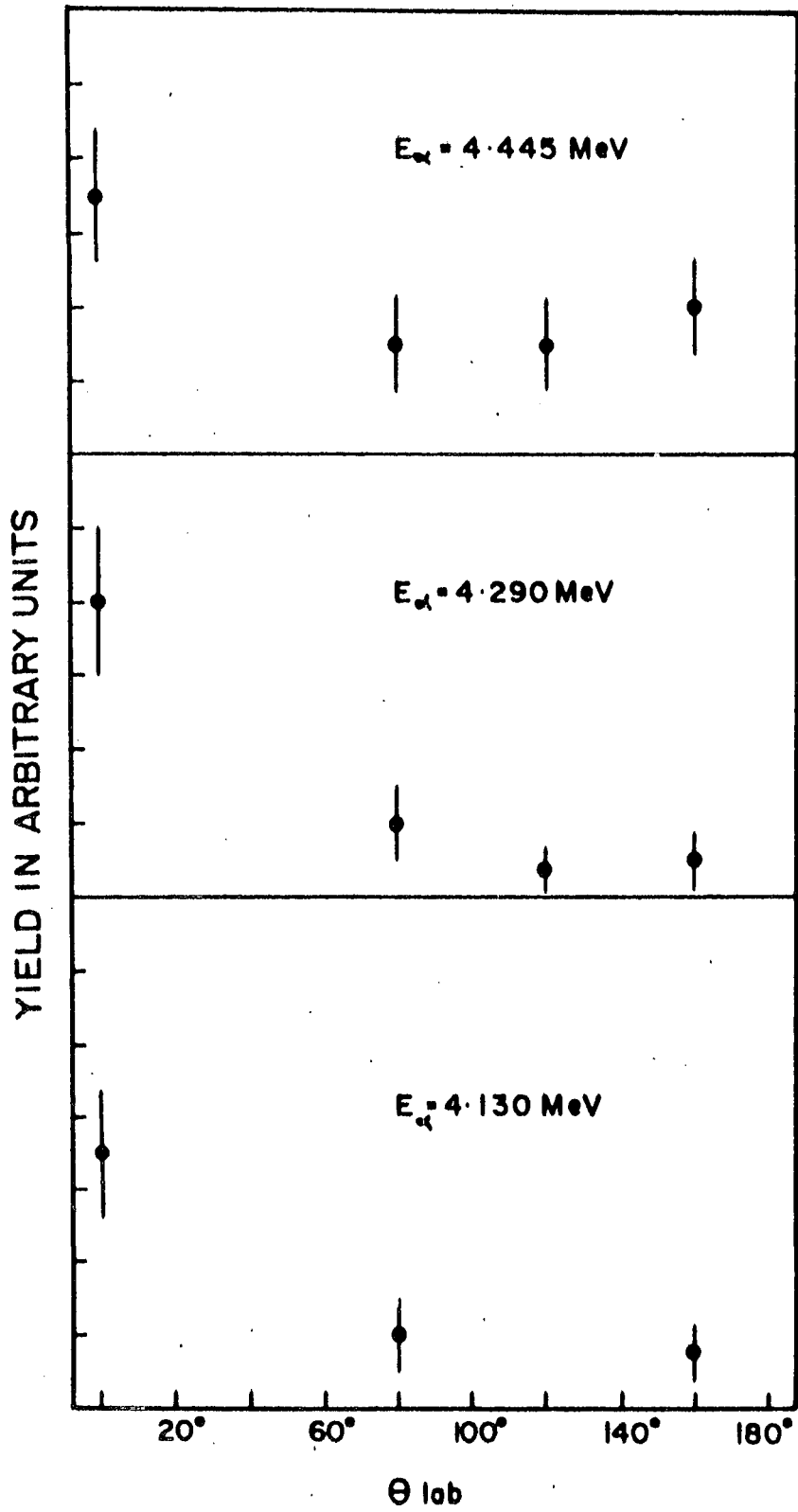


FIG. 23

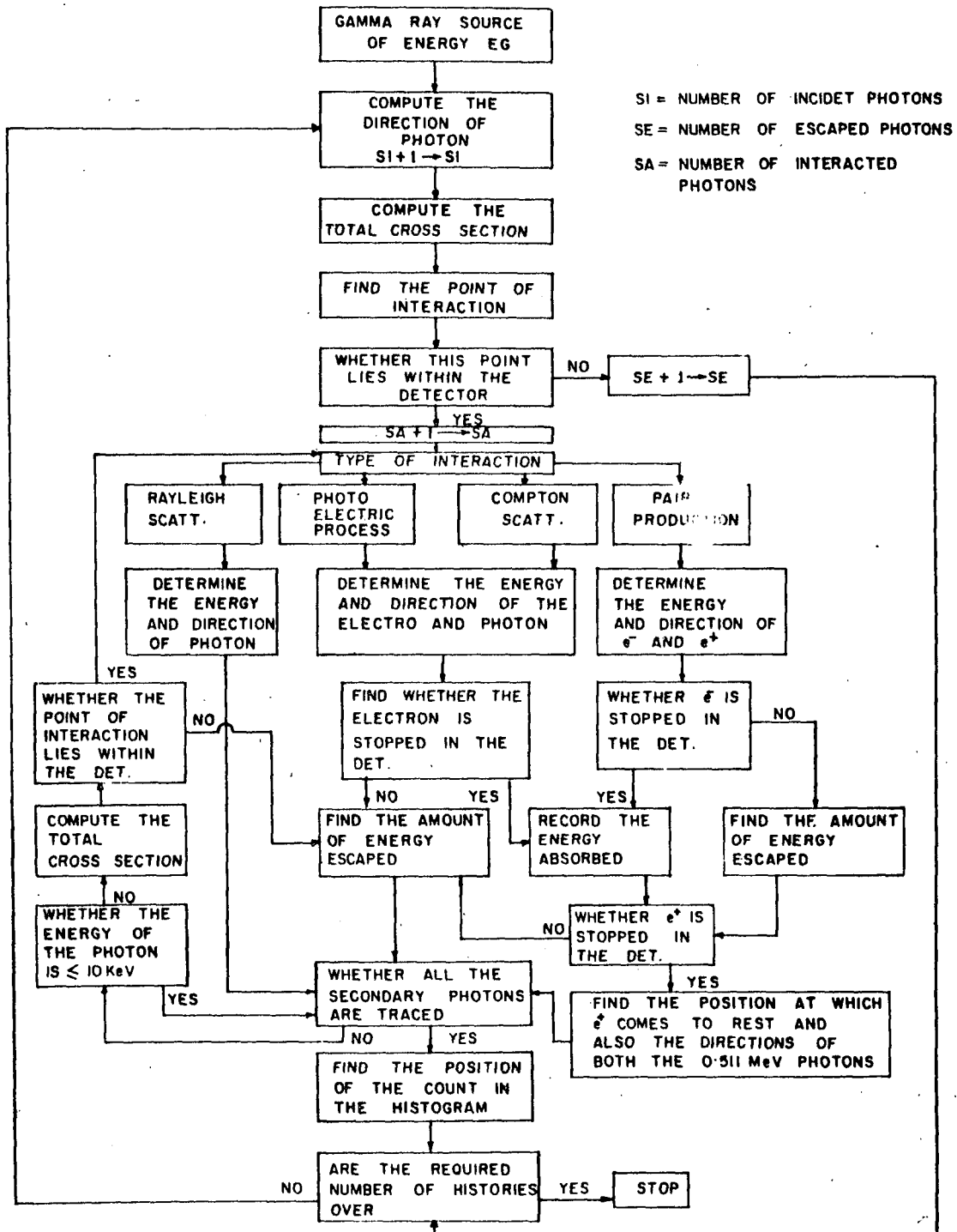


FIG. 24

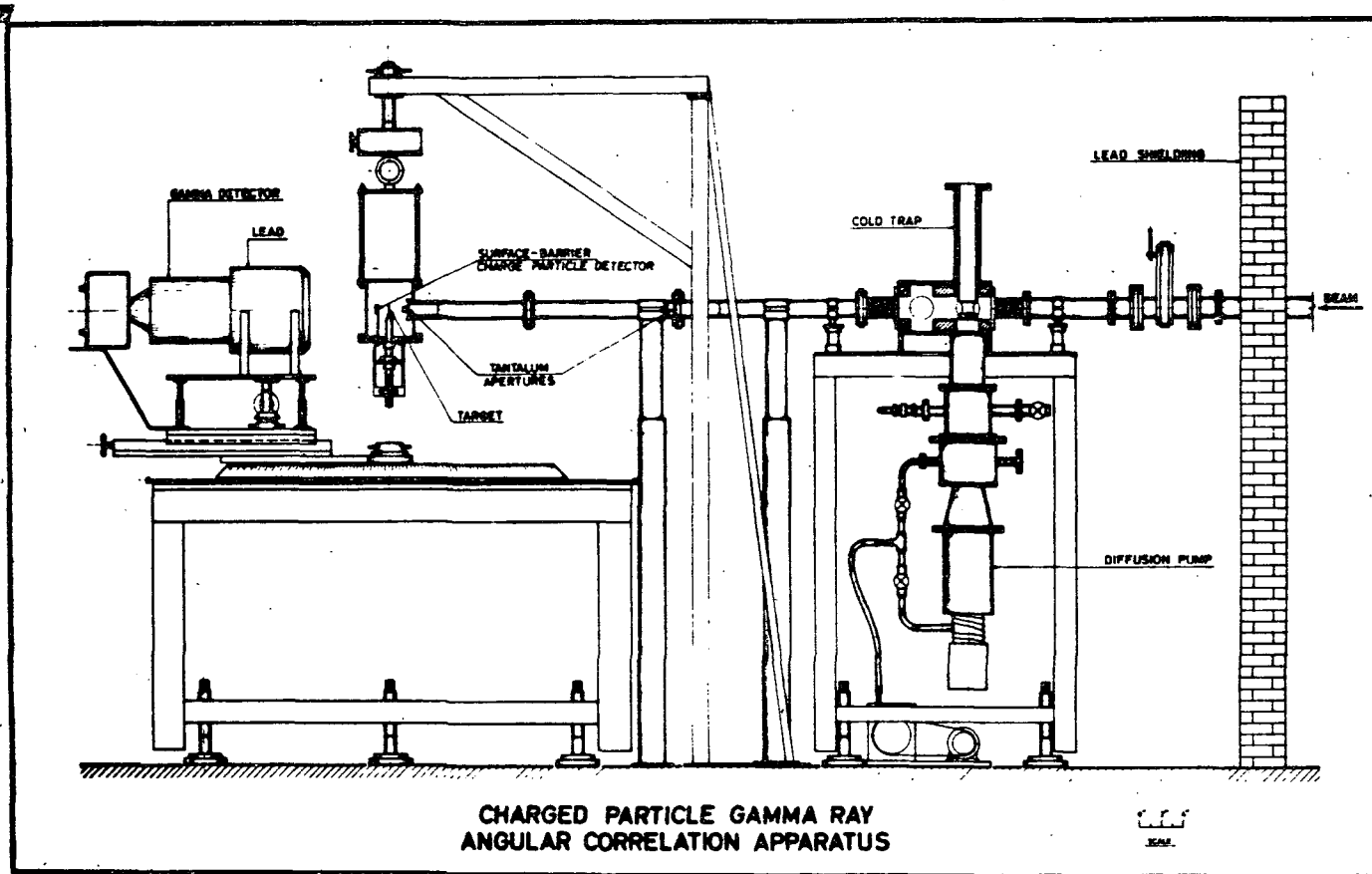


FIG-25

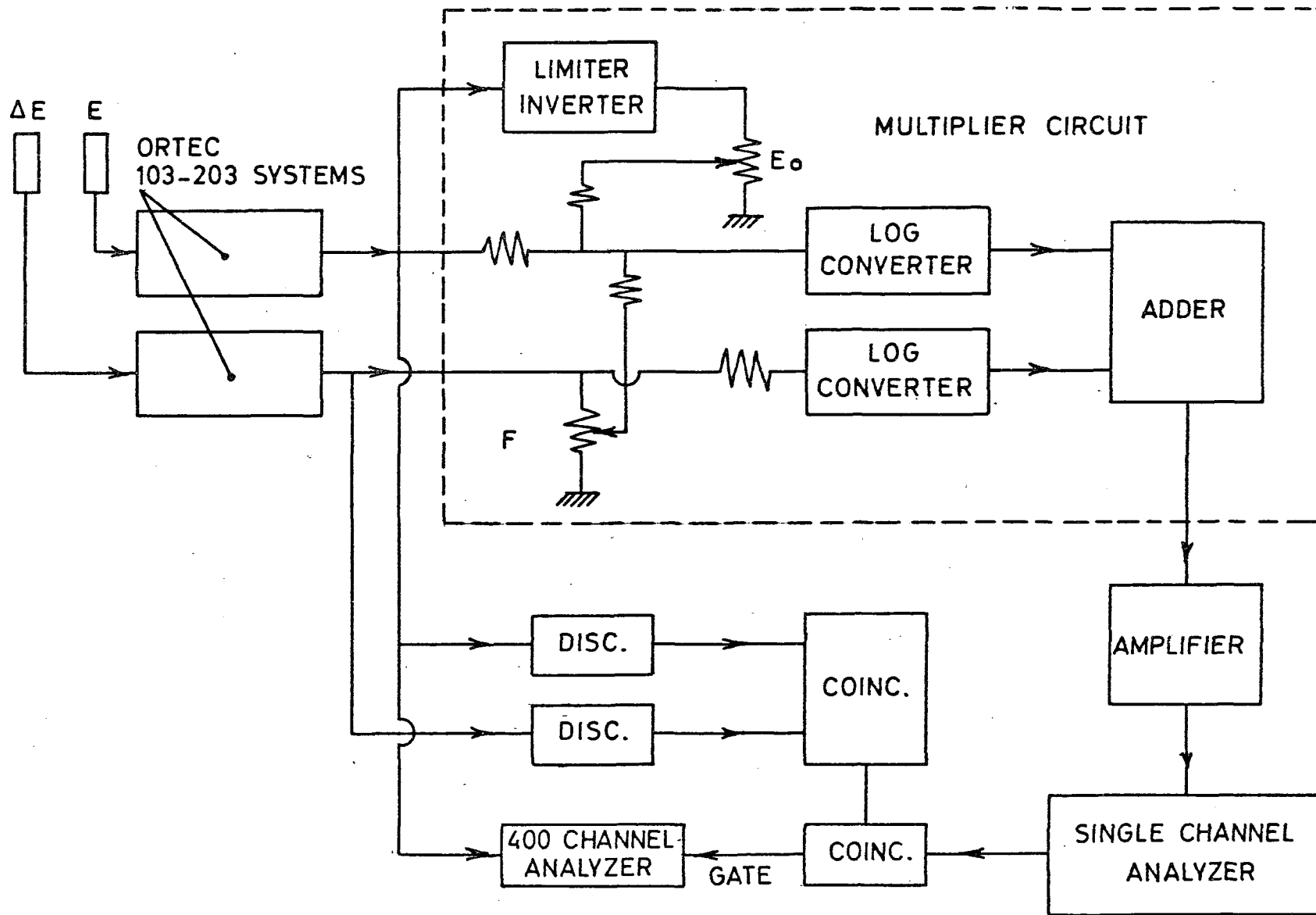


FIG. 26